

Chapter 4

Anisotropic anelastic media

... a single system of six mutually orthogonal types [strains] may be determined for any homogeneous elastic solid, so that its potential energy when homogeneously strained in any way is expressed by the sum of the products of the squares of the components of the strain, according to those types, respectively multiplied by six determinate coefficients [eigenstiffnesses]. The six strain-types thus determined are called the Six Principal Strain-types of the body. The coefficients ... are called the six Principal Elasticities of the body. If a body be strained to any of its six Principal Types, the stress required to hold it so is directly concurrent with [proportional to] the strain.

Lord Kelvin (Kelvin, 1856)

The so-called Neumann's principle (Neumann, 1885; Nye, 1987, p. 20) states, roughly speaking, that the symmetry of the consequences is at least as high as that of the causes. This implies that any kind of symmetry possessed by wave attenuation must be present within the crystallographic class of the material. This symmetry principle was clearly stated in 1884 by Pierre Curie in an article published in the *Bulletin de la Société Minéralogique de France*.

The quality factor or the related attenuation factor, which can be measured experimentally by various techniques (Toksöz and Johnston, 1981), quantifies dissipation in a given direction. Most experimental data about anisotropic attenuation are obtained in the laboratory at ultrasonic frequencies, but are not usually collected during seismic surveys. This lack of actual seismic data constitutes a serious problem because, unlike the slownesses, the attenuation behavior observed at ultrasonic frequency ranges cannot be extrapolated to the sonic and seismic ranges, since the mechanisms of dissipation can differ substantially in different frequency ranges.

Hosten, Deschamps and Tittmann (1987) measure the dependence of attenuation with propagation direction in a carbon-epoxy composite. They find that, in a sense, attenuation is more anisotropic than slowness, and while shear-wave dissipation is larger than longitudinal dissipation in the isotropy planes, the opposite behavior occurs in planes containing the axis of rotational symmetry. Arts, Rasolofosaon and Zinszner (1992) obtain the viscoelastic tensor of dry and saturated rock samples (sandstone and limestone). Their results indicate that attenuation in dry rocks is one order of magnitude lower than attenuation in saturated samples. Moreover, the attenuation is again more anisotropic than the slowness, a fact that Arts, Rasolofosaon and Zinszner interpret as attenuation

having lower symmetry than the slowness, or, alternatively, a consequence of experimental error. According to Baste and Audoin (1991), the elastic stiffnesses are quite adequate to describe the closing of cracks – provided that the proper experimental techniques are employed. On the other hand, laboratory data obtained by Yin (1993) on prestressed rocks suggest that attenuation may be more sensitive to the closing of cracks than the elastic stiffnesses, and that its symmetry is closely related to the type of loading. Yin finds a simple relation between wave amplitude and loading stress, and concludes that accurate estimates of wave attenuation can be used to quantify stress-induced anisotropy.

Since attenuation can be explained by many different mechanisms, it is difficult, if not impossible, to build a general microstructural theory. A phenomenological theory, such as viscoelasticity, leads to a convenient model. Although such a model does not allow us to predict attenuation levels, it can be used to estimate the anisotropy of attenuation. The problem is the determination of the time (or frequency) dependence of the relaxation tensor – 21 components in triclinic media. Most applications use the Kelvin-Voigt constitutive law, based on 21 independent viscosity functions (Lamb and Richter, 1966; Auld, 1990a, p. 101), corresponding to complex constants in the frequency domain. Occasionally, it has been possible to estimate all these constants satisfactorily (Hosten, Deschamps and Tittmann, 1987). This chapter presents alternative models based on fewer parameters, which are not the imaginary elasticity constants in themselves, but real quality factors – often more readily available in seismic practice. Moreover, we give a detailed description of the physical properties and energy associated with wave propagation in anisotropic anelastic media.

4.1 Stress-strain relations

Attenuation is a characteristic associated with a deformation state of the medium (e.g., a wave mode) and, therefore, a small number of parameters should suffice to obtain the relaxation components. In isotropic media, two – dilatational and shear – relaxation functions completely define the anelastic properties. For finely layered media, Backus averaging is a physically sound approach for obtaining the relaxation components of a transversely isotropic medium (referred to below as model 1; Carcione (1992c)). Two alternative constitutive laws (Carcione and Cavallini, 1994b, 1995d), not restricted to layered media, as is the Backus approach, relate waves and deformation modes to anelastic processes, using at most six relaxation functions. These laws are referred to as models 2 and 3.

We have seen in Section 2.1 (see equation (2.9)) that the stress-strain relation for an isothermal, anisotropic viscoelastic medium can be written as

$$\sigma_{ij}(\mathbf{x}, t) = \psi_{ijkl}(\mathbf{x}, t) * \partial_t \epsilon_{kl}(\mathbf{x}, t). \quad (4.1)$$

Using the shortened Voigt's notation, we note that

$$\boldsymbol{\sigma} = \boldsymbol{\Psi} * \partial_t \boldsymbol{\epsilon} \quad (4.2)$$

((equation (2.22)). Time-harmonic fields are represented by the real part of

$$[\cdot] \exp(i\omega t), \quad (4.3)$$

where $[\cdot]$ represents a complex vector that depends only on the spatial coordinates. Substituting the time dependence (4.3) into the stress-strain relations (4.2), we obtain

$$\boldsymbol{\sigma} = \mathbf{P} \cdot \mathbf{e}, \quad (\sigma_I = p_{IJ} e_J), \quad (4.4)$$

where

$$p_{IJ} = \int_{-\infty}^{\infty} \partial_t \psi_{IJ}(t) \exp(-i\omega t) dt \quad (4.5)$$

are the components of the stiffness matrix $\mathbf{P}(\mathbf{x}, \omega)$. For anelastic media, the components of \mathbf{P} are complex and frequency dependent. Note that the anelastic stress-strain relation discussed by Auld (1990a, p. 87) is a particular case of (4.4). Auld introduces a viscosity matrix $\boldsymbol{\eta}$ such that $\mathbf{P}(\omega) = \mathbf{C} + i\omega\boldsymbol{\eta}$, with \mathbf{C} being the low-frequency limit elasticity matrix. This equation corresponds to a Kelvin-Voigt stress-strain relation (see equation (2.161)).

We can use any complex moduli, satisfying the conditions listed in Section 2.2.5, to describe the anelastic properties of the medium. The simplest realistic model is a single Zener element (see Section 2.4.3) describing each anelastic deformation mode (identified by the index ν), whose (dimensionless) complex moduli can be expressed as

$$M_\nu(\omega) = \frac{\sqrt{Q_{0\nu}^2 + 1} - 1 + i\omega Q_{0\nu} \tau_0}{\sqrt{Q_{0\nu}^2 + 1} + 1 + i\omega Q_{0\nu} \tau_0}, \quad (4.6)$$

where the parameterization (2.200) and (2.202) is used. We shall see that depending on the symmetry class, the subscript ν goes from 1 to 6 at most. The quality factor Q_ν , associated with each modulus, is equal to the real part of M_ν divided by its imaginary part (see equation (2.120)). At $\omega_0 = 1/\tau_0$, the curve $Q_\nu(\omega)$ has its lowest value: $Q_\nu(\omega_0) = Q_{0\nu}$. The high-frequency limit corresponds to the elastic case, with $M_\nu \rightarrow 1$. Other complex moduli, other than (4.6), may also be appropriate, depending on the desired frequency dependence of attenuation¹.

Let us denote by c_{IJ} the elastic (or unrelaxed) stiffness constants. Then, $p_{IJ}(\omega \rightarrow \infty) = c_{IJ}$. Hooke's Law can be written either in the Voigt's notation as

$$\begin{pmatrix} \sigma_{11} \\ \sigma_{22} \\ \sigma_{33} \\ \sigma_{23} \\ \sigma_{13} \\ \sigma_{12} \end{pmatrix} = \begin{pmatrix} p_{11} & p_{12} & p_{13} & p_{14} & p_{15} & p_{16} \\ p_{12} & p_{22} & p_{23} & p_{24} & p_{25} & p_{26} \\ p_{13} & p_{23} & p_{33} & p_{34} & p_{35} & p_{36} \\ p_{14} & p_{24} & p_{34} & p_{44} & p_{45} & p_{46} \\ p_{15} & p_{25} & p_{35} & p_{45} & p_{55} & p_{56} \\ p_{16} & p_{26} & p_{36} & p_{46} & p_{56} & p_{66} \end{pmatrix} \cdot \begin{pmatrix} \epsilon_{11} \\ \epsilon_{22} \\ \epsilon_{33} \\ 2\epsilon_{23} \\ 2\epsilon_{13} \\ 2\epsilon_{12} \end{pmatrix}. \quad (4.7)$$

or in "Kelvin's notation" – required by model 2 below – as

$$\begin{pmatrix} \sigma_{11} \\ \sigma_{22} \\ \sigma_{33} \\ \sqrt{2}\sigma_{23} \\ \sqrt{2}\sigma_{13} \\ \sqrt{2}\sigma_{12} \end{pmatrix} = \begin{pmatrix} p_{11} & p_{12} & p_{13} & \sqrt{2}p_{14} & \sqrt{2}p_{15} & \sqrt{2}p_{16} \\ p_{12} & p_{22} & p_{23} & \sqrt{2}p_{24} & \sqrt{2}p_{25} & \sqrt{2}p_{26} \\ p_{13} & p_{23} & p_{33} & \sqrt{2}p_{34} & \sqrt{2}p_{35} & \sqrt{2}p_{36} \\ \sqrt{2}p_{14} & \sqrt{2}p_{24} & \sqrt{2}p_{34} & 2p_{44} & 2p_{45} & 2p_{46} \\ \sqrt{2}p_{15} & \sqrt{2}p_{25} & \sqrt{2}p_{35} & 2p_{45} & 2p_{55} & 2p_{56} \\ \sqrt{2}p_{16} & \sqrt{2}p_{26} & \sqrt{2}p_{36} & 2p_{46} & 2p_{56} & 2p_{66} \end{pmatrix} \cdot \begin{pmatrix} \epsilon_{11} \\ \epsilon_{22} \\ \epsilon_{33} \\ \sqrt{2}\epsilon_{23} \\ \sqrt{2}\epsilon_{13} \\ \sqrt{2}\epsilon_{12} \end{pmatrix}, \quad (4.8)$$

¹Use of the Kelvin-Voigt and constant- Q models require us to define the elastic case at a reference frequency, since the corresponding phase velocities tend to infinite at infinite frequency.

(Mehrabadi and Cowin, 1990; Helbig, 1994, p. 406), where the p_{IJ} are functions of c_{IJ} and M_ν . The three arrays in equation (4.8) are true tensors in 6-D space, while in equation (4.7) they are just arrays (Helbig, 1994, p. 406).

4.1.1 Model 1: Effective anisotropy

In Section 1.5, we showed that fine layering on a scale much finer than the dominant wavelength of the signal yields effective anisotropy (Backus, 1962). Carcione (1992c) uses this approach and the correspondence principle (see Section 3.6) to study the anisotropic characteristics of attenuation in viscoelastic finely layered media. In agreement with the theory developed in Sections 3.1 and 3.2, let each medium be isotropic and anelastic with complex Lamé parameters given by

$$\lambda(\omega) = \rho \left(c_P^2 - \frac{4}{3} c_S^2 \right) M_1(\omega) - \frac{2}{3} \rho c_S^2 M_2(\omega) \quad \text{and} \quad \mu(\omega) = \rho V_S^2 M_2(\omega), \quad (4.9)$$

(see Section 1.5), or

$$\mathcal{K} = \lambda + \frac{2}{3}\mu, \quad \text{and} \quad \mathcal{E} = \mathcal{K} + \frac{4}{3}\mu, \quad (4.10)$$

where M_1 and M_2 are the dilatational and shear complex moduli, respectively, c_P and c_S are the elastic high-frequency limit compressional and shear velocities, and ρ is the density. (In the work of Carcione (1992c), the relaxed moduli correspond to the elastic limit.) According to equation (1.188), the equivalent transversely isotropic medium is defined by the following complex stiffnesses:

$$\begin{aligned} p_{11} &= \langle \mathcal{E} - \lambda^2 \mathcal{E}^{-1} \rangle + \langle \mathcal{E}^{-1} \rangle^{-1} \langle \mathcal{E}^{-1} \lambda \rangle^2 \\ p_{33} &= \langle \mathcal{E}^{-1} \rangle^{-1} \\ p_{13} &= \langle \mathcal{E}^{-1} \rangle^{-1} \langle \mathcal{E}^{-1} \lambda \rangle \\ p_{55} &= \langle \mu^{-1} \rangle^{-1} \\ p_{66} &= \langle \mu \rangle, \end{aligned} \quad (4.11)$$

where $\langle \cdot \rangle$ denotes the thickness weighted average. In the case of a periodic sequence of two alternating layers, equations (4.11) are similar to those of Postma (1955).

4.1.2 Model 2: Attenuation via eigenstrains

We introduce now a stress-strain relation based on the fact that each eigenvector (called eigenstrain) of the stiffness tensor defines a fundamental deformation state of the medium (Kelvin, 1856; Helbig, 1994, p. 399). The six eigenvalues – called eigenstiffnesses – represent the genuine elastic parameters. For example, in the elastic case, the strain energy is uniquely parameterized by the six eigenstiffnesses. From this fact and the correspondence principle (see Section 3.6), we infer that in a real medium the rheological properties depend essentially on six relaxation functions, which are the generalization of the eigenstiffnesses to the viscoelastic case. The existence of six or less complex moduli depends on the symmetry class of the medium. This theory is developed in the work of Carcione and Cavallini (1994b). According to this approach, the principal steps in the construction of a viscoelastic rheology from a given elasticity tensor \mathbf{C} are the following:

1. Decompose the elasticity tensor, i.e., expressed in Kelvin's notation, as

$$\mathbf{C} = \sum_{I=1}^6 \Lambda_I \mathbf{e}_I \otimes \mathbf{e}_I, \quad (4.12)$$

where Λ_I and \mathbf{e}_I are the eigenvalues and normalized eigenvectors of \mathbf{C} , respectively; Λ_I and \mathbf{e}_I are real, because \mathbf{C} is a symmetric matrix.

2. Invoke the correspondence principle to obtain a straightforward viscoelastic generalization of the above equation for time-harmonic motions of angular frequency ω ,

$$\mathbf{P} = \sum_{I=1}^6 \Lambda_I^{(v)} \mathbf{e}_I \otimes \mathbf{e}_I, \quad \Lambda_I^{(v)} = \Lambda_I M_I(\omega), \quad (4.13)$$

where $M_I(\omega)$ are complex moduli, for instance, of the form (4.6). By construction, the eigenstiffnesses of \mathbf{P} are complex, but the eigenstrains are the same as those of \mathbf{C} and, hence, real.

The eigenstiffness and eigenstrains of materials of lower symmetry are given by Mehrabadi and Cowin (1990). The eigentensors may be represented as 3×3 symmetric matrices in 3-D space; therein, their eigenvalues are invariant under rotations and describe the magnitude of the deformation. Furthermore, their eigenvectors describe the orientation of the eigentensor in a given coordinate system. For instance, pure volume dilatations correspond to eigenstrains with three equal eigenvalues, and the trace of an isochoric eigenstrain is zero. Isochoric strains with two equal eigenvalues but opposite signs and a third eigenvalue of zero are plane shear tensors. To summarize, the eigentensors identify preferred modes of deformation associated with the particular symmetry of the material. An illustrative pictorial representation of these modes or eigenstrains has been designed by Helbig (1994, p. 451).

A given wave mode is characterized by its proper complex effective stiffness. This can be expressed and, hence, defined in terms of the complex eigenstiffnesses. For example, let us consider an isotropic viscoelastic solid. We have seen in section 1.1 that the total strain can be decomposed into the dilatational and deviatoric eigenstrains, whose eigenstiffnesses are related to the compressibility and shear moduli, respectively, the last with multiplicity five. Therefore, there are only two relaxation functions (or two complex eigenstiffnesses) in an isotropic medium: one describing pure dilatational anelastic behavior and the other describing pure shear anelastic behavior. Every eigenstress is directly proportional to its eigenstrain of identical form, the proportionality constant being the complex eigenstiffness.

For orthorhombic symmetry, the characteristic polynomial of the elasticity matrix, when in Kelvin's form, factors into the product of three linear factors and a cubic one. Therefore, eigenstiffnesses are found by resorting to Cardano's formulae. For a transversely isotropic medium, the situation is even simpler, as the characteristic polynomial factors into the product of two squared linear factors and a quadratic one. A straightforward computation then yields the independent entries of the complex stiffness matrix, in

Voigt's notation, namely,

$$\begin{aligned} p_{11} &= \Lambda_1^{(v)}(2+a^2)^{-1} + \Lambda_2^{(v)}(2+b^2)^{-1} + \Lambda_4^{(v)}/2 \\ p_{12} &= p_{11} - \Lambda_4^{(v)} \\ p_{33} &= a^2\Lambda_1^{(v)}(2+a^2)^{-1} + b^2\Lambda_2^{(v)}(2+b^2)^{-1} \\ p_{13} &= a\Lambda_1^{(v)}(2+a^2)^{-1} + b\Lambda_2^{(v)}(2+b^2)^{-1} \\ p_{55} &= \Lambda_3^{(v)}/2 \\ p_{66} &= \Lambda_4^{(v)}/2, \end{aligned} \quad (4.14)$$

where

$$a = \frac{4c_{13}}{c_{11} + c_{12} - c_{33} - \sqrt{c}}, \quad b = \frac{4c_{13}}{c_{11} + c_{12} - c_{33} + \sqrt{c}}, \quad (4.15)$$

and $\Lambda_I^{(v)}(\omega)$, $I = 1, \dots, 4$ are the complex and frequency-dependent eigenstiffnesses, given by

$$\begin{aligned} \Lambda_1^{(v)} &= \frac{1}{2}(c_{11} + c_{12} + c_{33} + \sqrt{c})M_1 \\ \Lambda_2^{(v)} &= \frac{1}{2}(c_{11} + c_{12} + c_{33} - \sqrt{c})M_2 \\ \Lambda_3^{(v)} &= 2c_{55}M_3 \\ \Lambda_4^{(v)} &= (c_{11} - c_{12})M_4, \end{aligned} \quad (4.16)$$

with

$$c = 8c_{13}^2 + (c_{11} + c_{12} - c_{33})^2. \quad (4.17)$$

The two-fold eigenstiffnesses Λ_3 and Λ_4 are related to pure “isochoric” eigenstrains, i.e., to volume-preserving changes of shape only, while the single eigenstiffnesses Λ_1 and Λ_2 are related to eigenstrains that consist of simultaneous changes in volume and shape. For relatively weak anisotropy, Λ_1 corresponds to a quasi-dilatational deformation and Λ_2 to a quasi-shear deformation. Moreover, Λ_3 and Λ_4 determine the Q values of the shear waves along the principal axes. This stress-strain relation can be implemented in a time-domain modeling algorithm with the use of Zener relaxation functions and the introduction of memory variables (Robertsson and Coates, 1997). At each time step, stresses and strain must be projected on the bases of the eigenstrains. These transformations increase the required number of computations compared to the approach presented in the next section.

4.1.3 Model 3: Attenuation via mean and deviatoric stresses

We design the constitutive law in such a way that M_1 is the dilatational modulus and M_2 , M_3 and M_4 are associated with shear deformations. In this stress-strain relation (Carcione, 1990; Carcione and Cavallini, 1995d), the mean stress (i.e., the trace of the stress tensor) is only affected by the dilatational complex modulus M_1 . Moreover, the deviatoric-stress components solely depend on the shear complex moduli, denoted by M_2 , M_3 and M_4 . The trace of the stress tensor is invariant under transformations of the coordinate system. This fact assures that the mean stress depends only on M_1 in any system.

The complex stiffnesses for an orthorhombic medium are given by

$$p_{I(I)} = c_{I(I)} - \bar{\mathcal{E}} + \bar{\mathcal{K}}M_1 + \frac{4}{3}\bar{\mu}M_\delta, \quad I = 1, 2, 3, \quad (4.18)$$

$$p_{IJ} = c_{IJ} - \bar{\mathcal{E}} + \bar{\mathcal{K}}M_1 + 2\bar{\mu} \left(1 - \frac{1}{3}M_\delta \right), \quad I, J = 1, 2, 3; \quad I \neq J, \quad (4.19)$$

$$p_{44} = c_{44}M_2, \quad p_{55} = c_{55}M_3, \quad p_{66} = c_{66}M_4, \quad (4.20)$$

where

$$\bar{\mathcal{K}} = \bar{\mathcal{E}} - \frac{4}{3}\bar{\mu} \quad (4.21)$$

and

$$\bar{\mathcal{E}} = \frac{1}{3} \sum_{I=1}^3 c_{II}, \quad \bar{\mu} = \frac{1}{3} \sum_{I=4}^6 c_{II}. \quad (4.22)$$

The index δ can be chosen to be 2, 3 or 4. Transverse isotropy requires $M_4 = M_3 = M_2$ and $p_{66} = c_{66} + \bar{\mu}(M_2 - 1)$.

The mean stress $\bar{\sigma} = \sigma_{ii}/3$ can be expressed in terms of the mean strain $\bar{\epsilon} = \epsilon_{ii}/3$ and strain components (1.2) as

$$\bar{\sigma} = \frac{1}{3}(c_{J1} + c_{J2} + c_{J3})e_J + 3\bar{\mathcal{K}}(M_1 - 1)\bar{\epsilon}, \quad (4.23)$$

which only depends on the dilatational complex modulus, as required above. Moreover, the deviatoric stresses are

$$\sigma_I - \bar{\sigma} = \sum_{K=1}^3 \left(\delta_{IK} - \frac{1}{3} \right) c_{KJ}e_J + 2\bar{\mu}(M_\delta - 1)(e_I - \bar{\epsilon}), \quad I \leq 3, \quad (4.24)$$

and

$$\sigma_I = \sum_{J=1}^3 c_{IJ}e_J + \sum_{J=4}^6 c_{IJ}M_{J-2}e_J, \quad I > 3, \quad (4.25)$$

which depend on the complex moduli associated with the quasi-shear mechanisms. This stress-strain relation has the advantage that the stiffnesses have a simple time-domain analytical form when using the Zener model. This permits the numerical solution of the visco-elastodynamic equations in the space-time domain (see Section 4.5). Examples illustrating the use of the three stress-strain relations are given in Carcione, Cavallini and Helbig (1998).

4.2 Wave velocities, slowness and attenuation vector

The dispersion relation for homogeneous viscoelastic plane waves has the form of the elastic dispersion relation, but the quantities involved are complex and frequency dependent. The generalization of equation (1.68) to the viscoelastic case, by using the correspondence principle (Section 3.6), can be written as

$$k^2 \boldsymbol{\Gamma} \cdot \mathbf{u} = \rho \omega^2 \mathbf{u}, \quad (k^2 \Gamma_{ij} u_j = \rho \omega^2 u_i), \quad (4.26)$$

where

$$\boldsymbol{\Gamma} = \mathbf{L} \cdot \mathbf{P} \cdot \mathbf{L}^\top, \quad (\Gamma_{ij} = l_{iI} p_{IJ} l_{Jj}). \quad (4.27)$$

The components of the Kelvin-Christoffel matrix Γ are given in equation (1.73), with the substitution of p_{IJ} for c_{IJ} . As in the isotropic case (see Section 3.3.1), the complex velocity is

$$v_c = \frac{\omega}{k}, \quad (4.28)$$

and the phase velocity is

$$\mathbf{v}_p = \left[\frac{\omega}{\operatorname{Re}(k)} \right] \hat{\boldsymbol{\kappa}} = \frac{\omega}{\kappa} = \left[\operatorname{Re} \left(\frac{1}{v_c} \right) \right]^{-1} \hat{\boldsymbol{\kappa}}. \quad (4.29)$$

Equation (4.26) constitutes an eigenequation

$$(\Gamma - \rho v_c^2 \mathbf{I}_3) \cdot \mathbf{u} = 0 \quad (4.30)$$

for the eigenvalues $(\rho v_c^2)_m$ and eigenvectors $(\mathbf{u})_m$, $m = 1, 2, 3$. The dispersion relation is then

$$\det(\Gamma - \rho v_c^2 \mathbf{I}_3) = 0, \quad (4.31)$$

or, using (4.28) and $k_i = k l_i$,

$$F(k_1, k_2, k_3, \omega) = 0. \quad (4.32)$$

The form (4.32) holds also for inhomogeneous plane waves.

The slowness, defined as the inverse of the phase velocity, is

$$\mathbf{s}_R = \left(\frac{1}{v_p} \right) \hat{\boldsymbol{\kappa}} = \operatorname{Re} \left(\frac{1}{v_c} \right) \hat{\boldsymbol{\kappa}}, \quad (4.33)$$

i.e., its magnitude is the real part of the complex slowness $1/v_c$.

According to the definition (3.26), the attenuation vector for homogeneous plane waves is

$$\boldsymbol{\alpha} = -\operatorname{Im}(\mathbf{k}) = -\omega \operatorname{Im} \left(\frac{1}{v_c} \right) \hat{\boldsymbol{\kappa}}. \quad (4.34)$$

The group-velocity vector is given by (1.126). Because an explicit real equation of the form $\omega = \omega(\kappa_1, \kappa_2, \kappa_3)$ is not available in general, we need to use implicit differentiation of the dispersion relation (4.32). For instance, for the x -component,

$$\frac{\partial \omega}{\partial \kappa_1} = \left(\frac{\partial \kappa_1}{\partial \omega} \right)^{-1}, \quad (4.35)$$

or, because $\kappa_1 = \operatorname{Re}(k_1)$,

$$\frac{\partial \omega}{\partial \kappa_1} = \left[\operatorname{Re} \left(\frac{\partial k_1}{\partial \omega} \right) \right]^{-1}. \quad (4.36)$$

Implicit differentiation of the complex dispersion relation (4.32) gives

$$\left(\frac{\partial F}{\partial \omega} \delta \omega + \frac{\partial F}{\partial k_1} \delta k_1 \right)_{k_2, k_3} = 0. \quad (4.37)$$

Then,

$$\left(\frac{\partial k_1}{\partial \omega} \right) = -\frac{\partial F / \partial \omega}{\partial F / \partial k_1}, \quad (4.38)$$

and similar results are obtained for the k_2 and k_3 components. Substituting the partial derivatives in equation (1.126), we can evaluate the group velocity as

$$\mathbf{v}_g = - \left[\operatorname{Re} \left(\frac{\partial F / \partial \omega}{\partial F / \partial k_1} \right) \right]^{-1} \hat{\mathbf{e}}_1 - \left[\operatorname{Re} \left(\frac{\partial F / \partial \omega}{\partial F / \partial k_2} \right) \right]^{-1} \hat{\mathbf{e}}_2 - \left[\operatorname{Re} \left(\frac{\partial F / \partial \omega}{\partial F / \partial k_3} \right) \right]^{-1} \hat{\mathbf{e}}_3, \quad (4.39)$$

which is a generalization of equation (1.130).

Finally, the velocity of the envelope of homogeneous plane waves has the same form (1.146) obtained for the anisotropic elastic case, where θ is the propagation – and attenuation – angle.

4.3 Energy balance and fundamental relations

The derivation of the energy-balance equation or Umov-Poynting theorem is straightforward when using complex notation. The basic equations for the time average of the different quantities involved in the energy-balance equation are (1.105) and (1.106). We also need to calculate the peak or maximum values of the physical quantities. We use the following property

$$\begin{aligned} [\operatorname{Re}(\mathbf{a}^\top) \cdot \operatorname{Re}(\mathbf{b})]_{\text{peak}} &= \frac{1}{2} [|a_k| |b_k| \cos(\arg(\mathbf{a}_k) - \arg(\mathbf{b}_k)) + \\ &\sqrt{|a_k| |b_k| |a_j| |b_j| \cos(\arg(\mathbf{a}_k) + \arg(\mathbf{b}_k) - \arg(\mathbf{a}_j) + \arg(\mathbf{b}_j))}], \end{aligned} \quad (4.40)$$

where $|a_k|$ is the magnitude of the k -component of the field variable \mathbf{a} , and implicit summation over repeated indices is assumed (Carcione and Cavallini, 1993). When, for every k , $\arg(\mathbf{a}_k) = \phi_a$ and $\arg(\mathbf{b}_k) = \phi_b$, i.e., all the components of each variable are in phase, equation (4.40) reduces to

$$[\operatorname{Re}(\mathbf{a}^\top) \cdot \operatorname{Re}(\mathbf{b})]_{\text{peak}} = |a_k| |b_k| \cos \left(\frac{\phi_a - \phi_b}{2} \right), \quad (4.41)$$

and if, moreover, $\mathbf{a} = \mathbf{b}$, then

$$[\operatorname{Re}(\mathbf{a}^\top) \cdot \operatorname{Re}(\mathbf{b})]_{\text{peak}} = 2 \langle \operatorname{Re}(\mathbf{a}^\top) \cdot \operatorname{Re}(\mathbf{a}) \rangle. \quad (4.42)$$

When all the components of \mathbf{a} are in phase,

$$\langle \operatorname{Re}(\mathbf{a}^\top) \cdot \operatorname{Re}(\mathbf{D}) \cdot \operatorname{Re}(\mathbf{a}) \rangle_{\text{peak}} = 2 \langle \operatorname{Re}(\mathbf{a}^\top) \cdot \operatorname{Re}(\mathbf{D}) \cdot \operatorname{Re}(\mathbf{a}) \rangle \quad (4.43)$$

(Carcione and Cavallini, 1993, 1995a).

For time-harmonic fields of angular frequency ω , the strain/particle-velocity relation (1.26) and the equation of momentum conservation (1.28) can be expressed as

$$i\omega \mathbf{e} = \nabla^\top \cdot \mathbf{v} \quad (4.44)$$

and

$$\nabla \cdot \boldsymbol{\sigma} = i\omega \rho \mathbf{v} - \mathbf{f}, \quad (4.45)$$

where \mathbf{v} is the particle-velocity vector.

To derive the balance equation, the dot product of the equation of motion (4.45) is first taken with $-\mathbf{v}^*$ to give

$$-\mathbf{v}^* \cdot \nabla \cdot \boldsymbol{\sigma} = -i\omega\rho\mathbf{v}^* \cdot \mathbf{v} + \mathbf{v}^* \cdot \mathbf{f}. \quad (4.46)$$

On the other hand, the dot product of $-\boldsymbol{\sigma}^\top$ with the complex conjugate of (4.44) is

$$-\boldsymbol{\sigma}^\top \cdot \nabla^\top \cdot \mathbf{v}^* = i\omega\boldsymbol{\sigma}^\top \cdot \mathbf{e}^*. \quad (4.47)$$

Adding equations (4.46) and (4.47), we get

$$-\mathbf{v}^* \cdot \nabla \cdot \boldsymbol{\sigma} - \boldsymbol{\sigma}^\top \cdot \nabla^\top \cdot \mathbf{v}^* = -i\omega\rho\mathbf{v}^* \cdot \mathbf{v} + i\omega\boldsymbol{\sigma}^\top \cdot \mathbf{e}^* + \mathbf{v}^* \cdot \mathbf{f}. \quad (4.48)$$

The left-hand side of (4.48) is simply

$$-\mathbf{v}^* \cdot \nabla \cdot \boldsymbol{\sigma} - \boldsymbol{\sigma}^\top \cdot \nabla^\top \cdot \mathbf{v}^* = -\text{div}(\boldsymbol{\Sigma} \cdot \mathbf{v}^*), \quad (4.49)$$

where $\boldsymbol{\Sigma}$ is the 3×3 stress tensor defined in equation (1.108). Then, equation (4.48) can be expressed as

$$-\frac{1}{2}\text{div}(\boldsymbol{\Sigma} \cdot \mathbf{v}^*) = -i\omega\frac{1}{2}\rho\mathbf{v}^* \cdot \mathbf{v} + i\omega\frac{1}{2}\boldsymbol{\sigma}^\top \cdot \mathbf{e}^* + \frac{1}{2}\mathbf{v}^* \cdot \mathbf{f}. \quad (4.50)$$

After substitution of the stress-strain relation (4.4), equation (4.50) gives

$$-\frac{1}{2}\text{div}(\boldsymbol{\Sigma} \cdot \mathbf{v}^*) = 2i\omega \left[-\frac{1}{4}\rho\mathbf{v}^* \cdot \mathbf{v} + \frac{1}{4}\text{Re}(\mathbf{e}^\top \cdot \mathbf{P} \cdot \mathbf{e}^*) \right] - \frac{\omega}{2}\text{Im}(\mathbf{e}^\top \cdot \mathbf{P} \cdot \mathbf{e}^*) + \frac{1}{2}\mathbf{v}^* \cdot \mathbf{f}. \quad (4.51)$$

The significance of this equation becomes clear when we recognize that each of its terms has a precise physical meaning on a time-average basis. For instance, from equation (1.105),

$$\frac{1}{4}\rho\mathbf{v}^* \cdot \mathbf{v} = \frac{1}{2}\rho\langle\text{Re}(\mathbf{v}) \cdot \text{Re}(\mathbf{v})\rangle = \langle T \rangle \quad (4.52)$$

is the time-averaged kinetic-energy density; from (1.106)

$$\frac{1}{4}\text{Re}(\mathbf{e}^\top \cdot \mathbf{P} \cdot \mathbf{e}^*) = \frac{1}{2}\langle\text{Re}(\mathbf{e}^\top) \cdot \text{Re}(\mathbf{P}) \cdot \text{Re}(\mathbf{e})\rangle = \langle V \rangle \quad (4.53)$$

is the time-averaged strain-energy density, and

$$\frac{\omega}{2}\text{Im}(\mathbf{e}^\top \cdot \mathbf{P} \cdot \mathbf{e}^*) = \frac{\omega}{2}\langle\text{Re}(\mathbf{e}^\top) \cdot \text{Im}(\mathbf{P}) \cdot \text{Re}(\mathbf{e})\rangle = \langle \dot{D} \rangle \quad (4.54)$$

is the time-averaged rate of dissipated-energy density. Because the strain energy and the rate of dissipated energies should always be positive, $\text{Re}(\mathbf{P})$ and $\text{Im}(\mathbf{P})$ must be positive definite matrices (see Holland, 1967). These conditions are the generalization of the condition of stability discussed in Section 1.2. If expressed in terms of the eigenvalues of matrix \mathbf{P} (see Section 4.1.2)), the real and imaginary parts of these eigenvalues must be positive. It can be shown that the three models introduced in Section 4.1 satisfy the stability conditions (see Carcione (1990) for a discussion of model 3).

The complex power-flow vector or Umov-Poynting vector is defined as

$$\mathbf{p} = -\frac{1}{2}\boldsymbol{\Sigma} \cdot \mathbf{v}^* \quad (4.55)$$

and

$$p_s = \frac{1}{2} \mathbf{v}^* \cdot \mathbf{f} \quad (4.56)$$

is the complex power per unit volume supplied by the body forces. Substituting the preceding expressions into equation (4.51), we obtain the energy-balance equation

$$\operatorname{div} \mathbf{p} - 2i\omega(\langle V \rangle - \langle T \rangle) + \langle \dot{D} \rangle = p_s. \quad (4.57)$$

The time-averaged energy density is

$$\langle E \rangle = \langle T \rangle + \langle V \rangle = \frac{1}{4} [\rho \mathbf{v}^* \cdot \mathbf{v} + \operatorname{Re}(\mathbf{e}^\top \cdot \mathbf{P} \cdot \mathbf{e}^*)]. \quad (4.58)$$

In lossless media, $\langle \dot{D} \rangle = 0$, and because in the absence of sources the net energy flow into or out of a given closed surface must vanish, $\operatorname{div} \mathbf{p} = 0$. Thus, the average kinetic energy equals the average strain energy. As a consequence, the average stored energy is twice the average strain energy.

By separating the real and imaginary parts of equation (4.57), two independent and separately meaningful physical relations are obtained:

$$-\operatorname{Re}(\operatorname{div} \mathbf{p}) + \operatorname{Re}(p_s) = \langle \dot{D} \rangle \quad (4.59)$$

and

$$-\operatorname{Im}(\operatorname{div} \mathbf{p}) + \operatorname{Im}(p_s) = 2\omega(\langle T \rangle - \langle V \rangle). \quad (4.60)$$

For linearly polarized fields, the components of the particle-velocity vector \mathbf{v} are in phase, and the average kinetic energy is half the peak kinetic energy by virtue of equation (4.42). The same property holds for the strain energy if the components of the strain array \mathbf{e} are in phase (see equation (4.43)). In this case, the energy-balance equation reads

$$\operatorname{div} \mathbf{p} - i\omega(\langle V \rangle_{\text{peak}} - \langle T \rangle_{\text{peak}}) + \langle \dot{D} \rangle = p_s, \quad (4.61)$$

in agreement with Auld (1990a, p. 154). Equation (4.61) is found to be valid only for homogeneous viscoelastic plane waves, i.e., when the propagation direction coincides with the attenuation direction, although Auld (1990a, eq. 5.76) seems to attribute a general validity to that equation. Notably, it should be pointed out that for inhomogeneous viscoelastic plane waves, the peak value is not twice the average value. The same remark applies to Ben-Menahem and Singh (1981, p. 883).

4.3.1 Plane waves. Energy velocity and quality factor

A general solution representing inhomogeneous viscoelastic plane waves is of the form

$$[\cdot] \exp[i(\omega t - \mathbf{k} \cdot \mathbf{x})], \quad (4.62)$$

where $[\cdot]$ is a constant complex vector. The wavevector is complex and can be written as in equation (3.26), with $\boldsymbol{\kappa} \cdot \boldsymbol{\alpha}$ strictly different from zero, unlike the interface waves in elastic media. For these plane waves, the operator (1.25) takes the form

$$\nabla \rightarrow -i\mathbf{K}, \quad (4.63)$$

where

$$\mathbf{K} = \begin{pmatrix} k_1 & 0 & 0 & 0 & k_3 & k_2 \\ 0 & k_2 & 0 & k_3 & 0 & k_1 \\ 0 & 0 & k_3 & k_2 & k_1 & 0 \end{pmatrix}, \quad (4.64)$$

with k_1 , k_2 and k_3 being the components of the complex wavevector \mathbf{k} . Note that for the corresponding conjugated fields, the operator should be replaced by $i\mathbf{K}^*$.

Substituting the differential operator ∇ into equations (4.46) and (4.47) and assuming $\mathbf{f} = 0$, we obtain

$$\mathbf{v}^* \cdot \mathbf{K} \cdot \boldsymbol{\sigma} = -\omega \rho \mathbf{v}^* \cdot \mathbf{v}^* \quad (4.65)$$

and

$$\boldsymbol{\sigma}^\top \cdot \mathbf{K}^{*\top} \cdot \mathbf{v}^* = -\omega \boldsymbol{\sigma}^\top \cdot \mathbf{e}^*, \quad (4.66)$$

respectively. From equation (4.4), the right-hand side of (4.66) gives

$$-\omega \boldsymbol{\sigma}^\top \cdot \mathbf{e}^* = -\omega \mathbf{e}^\top \cdot \mathbf{P} \cdot \mathbf{e}^*, \quad (4.67)$$

since \mathbf{P} is symmetric. The left-hand sides of (4.65) and (4.66) contain the Umov-Poynting vector (4.55) because $\mathbf{K} \cdot \boldsymbol{\sigma} = \boldsymbol{\Sigma} \cdot \mathbf{k}$ and $\mathbf{K}^* \cdot \boldsymbol{\sigma} = \boldsymbol{\Sigma} \cdot \mathbf{k}^*$; thus

$$2\mathbf{k} \cdot \mathbf{p} = \omega \rho \mathbf{v}^* \cdot \mathbf{v} \quad (4.68)$$

and

$$2\mathbf{k}^* \cdot \mathbf{p} = \omega \mathbf{e}^\top \cdot \mathbf{P} \cdot \mathbf{e}^*. \quad (4.69)$$

In terms of the energy densities (4.52), (4.53) and (4.54),

$$\mathbf{k} \cdot \mathbf{p} = 2\omega \langle T \rangle \quad (4.70)$$

and

$$\mathbf{k}^* \cdot \mathbf{p} = 2\omega \langle V \rangle + i\langle \dot{D} \rangle. \quad (4.71)$$

Because the right-hand side of (4.70) is real, the product $\mathbf{k} \cdot \mathbf{p}$ is also real. For elastic (lossless) media, \mathbf{k} and the Umov-Poynting vectors are both real quantities.

Adding equations (4.70) and (4.71) and using $\mathbf{k}^* + \mathbf{k} = 2\boldsymbol{\kappa}$, with $\boldsymbol{\kappa}$ being the real wavevector (see equation (3.26)), we obtain

$$\boldsymbol{\kappa} \cdot \mathbf{p} = \omega \langle E \rangle + \frac{i}{2} \langle \dot{D} \rangle, \quad (4.72)$$

where the time-averaged energy density (4.58) has been used to obtain (4.72). Splitting equation (4.72) into real and imaginary parts, we have

$$\boldsymbol{\kappa} \cdot \langle \mathbf{p} \rangle = \omega \langle E \rangle \quad (4.73)$$

and

$$\boldsymbol{\kappa} \cdot \text{Im}(\mathbf{p}) = \frac{1}{2} \langle \dot{D} \rangle, \quad (4.74)$$

where

$$\langle \mathbf{p} \rangle = \text{Re}(\mathbf{p}) \quad (4.75)$$

is the average power-flow density. The energy-velocity vector is defined as

$$\mathbf{v}_e = \frac{\langle \mathbf{p} \rangle}{\langle E \rangle} = \frac{\langle \mathbf{p} \rangle}{\langle T + V \rangle}, \quad (4.76)$$

which defines the location of the wave surface associated with each Fourier component, i.e., with each frequency ω . In lossy media, we define the wave front as the wave surface corresponding to infinite frequency, since the unrelaxed energy velocity is greater than the relaxed energy velocity.

Since the phase velocity is

$$\mathbf{v}_p = \left(\frac{\omega}{\kappa} \right) \hat{\boldsymbol{\kappa}}, \quad (4.77)$$

where $\hat{\boldsymbol{\kappa}}$ defines the propagation direction, the following relation is obtained from (4.73):

$$\hat{\boldsymbol{\kappa}} \cdot \mathbf{v}_e = v_p. \quad (4.78)$$

This relation, as in the lossless case (equation (1.114)) and the isotropic viscoelastic case (equation (3.123)), means that the phase velocity is the projection of the energy velocity onto the propagation direction. Note also that equation (4.74) can be written as

$$\hat{\boldsymbol{\kappa}} \cdot \mathbf{v}_d = v_p, \quad (4.79)$$

where \mathbf{v}_d is a velocity defined as

$$\mathbf{v}_d = \frac{2\omega \text{Im}(\mathbf{p})}{\langle \dot{D} \rangle}, \quad (4.80)$$

and associated with the rate of dissipated-energy density. Relations (4.78) and (4.79) are illustrated in Figure 4.1.

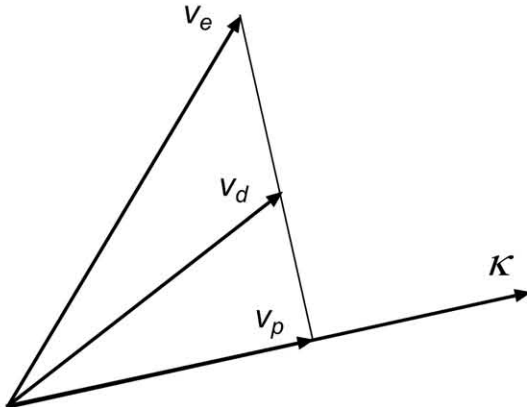


Figure 4.1: Graphical representation of equations (4.78) and (4.79). The projection of the energy-velocity vector onto the propagation direction gives the phase velocity. The same result is obtained by the projection of a pseudo-velocity vector related to the dissipated energy.

Another important relation obtained from equation (4.73) is

$$\langle E \rangle = \frac{1}{\omega} \boldsymbol{\kappa} \cdot \langle \mathbf{p} \rangle, \quad (4.81)$$

which means that the time-averaged energy density can be computed from the component of the average power-flow vector along the propagation direction.

Subtracting (4.71) from (4.70), we get

$$-2\boldsymbol{\alpha} \cdot \mathbf{p} = 2i\omega(\langle V \rangle - \langle T \rangle) - \langle \dot{D} \rangle, \quad (4.82)$$

which can also be deduced from the energy-balance equation (4.57), since for plane waves of the form (4.62), $\operatorname{div} \mathbf{p} = -2\boldsymbol{\alpha} \cdot \mathbf{p}$. Taking the real part of (4.82), we have

$$\langle \dot{D} \rangle = 2\boldsymbol{\alpha} \cdot \langle \mathbf{p} \rangle, \quad (4.83)$$

which states that the time average of the rate of dissipated-energy density can be obtained from the projection of the average power-flow vector onto the attenuation direction. Relations (4.81) and (4.83) are illustrated in Figure 4.2.

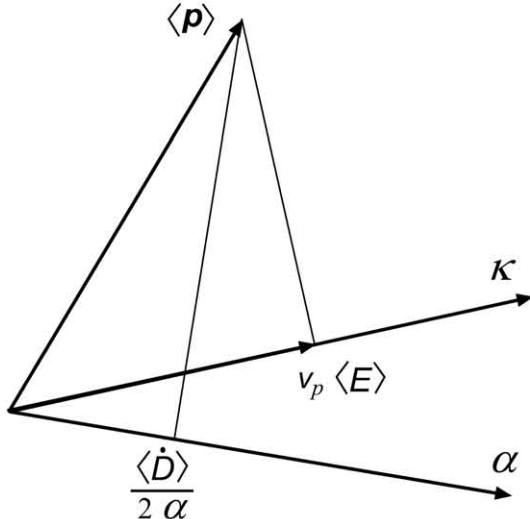


Figure 4.2: Graphical representation of equations (4.81) and (4.83). The time-averaged energy density can be calculated as the component of the average power-flow vector onto the propagation direction, while the time average of the rate of dissipated-energy density depends on the projection of the average power-flow vector onto the attenuation direction.

We define the quality factor as in the 1-D and isotropic cases (equations (2.119) and (3.126), respectively); that is

$$Q = \frac{2\langle V \rangle}{\langle D \rangle}, \quad (4.84)$$

where

$$\langle D \rangle \equiv \omega^{-1} \langle \dot{D} \rangle \quad (\omega > 0) \quad (4.85)$$

is the time-averaged dissipated-energy density. Substituting the time-averaged strain-energy density (4.53) and the time-averaged dissipated energy (4.85) into equation (4.84) and using (4.54), we obtain

$$Q = \frac{\operatorname{Re}(\mathbf{e}^\top \cdot \mathbf{P} \cdot \mathbf{e}^*)}{\operatorname{Im}(\mathbf{e}^\top \cdot \mathbf{P} \cdot \mathbf{e}^*)}. \quad (4.86)$$

This equation requires the calculation of $\mathbf{e}^\top \cdot \mathbf{P} \cdot \mathbf{e}^*$.

For homogeneous plane waves and using equation (1.26), we obtain

$$\mathbf{e} = -ik\mathbf{L}^\top \cdot \mathbf{u} \quad (4.87)$$

and

$$\mathbf{e}^* = ik^*\mathbf{L}^\top \cdot \mathbf{u}^*, \quad (4.88)$$

where \mathbf{L} is defined in equation (1.67). Replacing these expressions in $\mathbf{e}^\top \cdot \mathbf{P} \cdot \mathbf{e}^*$, we get

$$\mathbf{e}^\top \cdot \mathbf{P} \cdot \mathbf{e}^* = |k|^2 \mathbf{u} \cdot \boldsymbol{\Gamma} \cdot \mathbf{u}^*, \quad (4.89)$$

where $\boldsymbol{\Gamma}$ is the Kelvin-Christoffel matrix (4.27). But from the transpose of (4.30),

$$\mathbf{u} \cdot \boldsymbol{\Gamma} = \rho v_c^2 \mathbf{u}. \quad (4.90)$$

Therefore, the substitution of this expression into (4.89) gives

$$\mathbf{e}^\top \cdot \mathbf{P} \cdot \mathbf{e}^* = \rho |k|^2 v_c^2 \mathbf{u} \cdot \mathbf{u}^* = \rho |k|^2 v_c^2 |\mathbf{u}|^2. \quad (4.91)$$

Consequently, substituting this expression into equation (4.86), the quality factor for homogeneous plane waves in anisotropic viscoelastic media takes the following simple form as a function of the complex velocity:

$$Q = \frac{\operatorname{Re}(v_c^2)}{\operatorname{Im}(v_c^2)}. \quad (4.92)$$

The relation (3.128) and the approximation (3.129), obtained for isotropic media, are also valid in this case. Similarly, because for a homogeneous wave $k^2 = \kappa^2 - \alpha^2 - 2i\kappa\alpha$, it follows from (4.34) and (3.126) that the quality factor relates to the wavenumber and attenuation vectors as

$$\boldsymbol{\alpha} = \left(\sqrt{Q^2 + 1} - Q \right) \boldsymbol{\kappa}. \quad (4.93)$$

For low-loss solids, the quality factor is $Q \gg 1$, and a Taylor expansion yields

$$\boldsymbol{\alpha} = \frac{1}{2Q} \boldsymbol{\kappa}, \quad (4.94)$$

which is equivalent to equation (3.129).

4.3.2 Polarizations

We have shown in Section 3.3.4, that in isotropic media the polarizations of P and S-I homogeneous planes waves can be orthogonal under certain conditions. In anisotropic anelastic media, the symmetry of the Kelvin-Christoffel matrix Γ (equation (4.27)) implies the orthogonality – in the complex sense – of the eigenvectors associated with the three homogeneous plane-wave modes. (This can be shown by using the same steps followed in Section 1.3.3). Let us assume that Γ has three distinct eigenvalues and denote two of the corresponding eigenvectors by \mathbf{u}_a and \mathbf{u}_b . Orthogonality implies

$$\mathbf{u}_a \cdot \mathbf{u}_b = 0, \quad (4.95)$$

or

$$\text{Re}(\mathbf{u}_a) \cdot \text{Re}(\mathbf{u}_b) - \text{Im}(\mathbf{u}_a) \cdot \text{Im}(\mathbf{u}_b) = 0. \quad (4.96)$$

This condition does not imply orthogonality of the polarizations, i.e., $\text{Re}(\mathbf{u}_a) \cdot \text{Re}(\mathbf{u}_b) \neq 0$.

The real displacement vector of an inhomogeneous plane wave can be expressed as

$$\text{Re}(\mathbf{u}) = U_0 \text{Re}\{\mathbf{U} \exp[i(\omega t - \mathbf{k} \cdot \mathbf{x})]\}, \quad (4.97)$$

where U_0 is a real quantity, and \mathbf{U} can be normalized in the Hermitian sense; that is

$$\mathbf{U} \cdot \mathbf{U}^* = 1. \quad (4.98)$$

Decomposing the complex vectors into their real and imaginary parts and using $\mathbf{k} = \boldsymbol{\kappa} - i\boldsymbol{\alpha}$, we obtain:

$$\text{Re}(\mathbf{u}) = U_0 \exp(-\boldsymbol{\alpha} \cdot \mathbf{x}) [\text{Re}(\mathbf{U}) \cos \varsigma - \text{Im}(\mathbf{U}) \sin \varsigma], \quad (4.99)$$

where

$$\varsigma = \omega t - \boldsymbol{\kappa} \cdot \mathbf{x}. \quad (4.100)$$

The displacement vector describes an ellipse homothetic² to the ellipse defined by

$$\mathbf{w} = \text{Re}(\mathbf{U}) \cos \varsigma - \text{Im}(\mathbf{U}) \sin \varsigma. \quad (4.101)$$

Let us consider two displacement vectors \mathbf{w}_a and \mathbf{w}_b associated with two different wave modes at the same time and at the same frequency. The scalar product between those displacements is

$$\begin{aligned} \mathbf{w}_a \cdot \mathbf{w}_b &= \text{Re}(\mathbf{U}_a) \cdot \text{Re}(\mathbf{U}_b) \cos(\varsigma_a) \cos(\varsigma_b) + \text{Im}(\mathbf{U}_a) \cdot \text{Im}(\mathbf{U}_b) \sin(\varsigma_a) \sin(\varsigma_b) \\ &\quad - \text{Im}(\mathbf{U}_a) \cdot \text{Re}(\mathbf{U}_b) \sin(\varsigma_a) \cos(\varsigma_b) - \text{Re}(\mathbf{U}_a) \cdot \text{Im}(\mathbf{U}_b) \cos(\varsigma_a) \sin(\varsigma_b). \end{aligned} \quad (4.102)$$

Using the condition (4.95), which holds for homogeneous waves, equation (4.102) simplifies to

$$\mathbf{w}_a \cdot \mathbf{w}_b = \text{Re}(\mathbf{U}_a) \cdot \text{Re}(\mathbf{U}_b) \cos(\varsigma_a - \varsigma_b) + \text{Re}(\mathbf{U}_a) \cdot \text{Im}(\mathbf{U}_b) \sin(\varsigma_a - \varsigma_b), \quad (4.103)$$

but it is not equal to zero. In general, the planes of the three elliptical polarizations are not mutually perpendicular. See Arts (1993) for an analysis of the characteristics of the elliptical motion associated with (4.101).

²Two figures are homothetic if they are related by an expansion or a geometric contraction.

4.4 The physics of wave propagation for viscoelastic SH waves

We have seen in Chapter 1 that in anisotropic lossless media, the energy, group and envelope velocities coincide, but the energy velocity is not equal to the phase velocity. On the other hand, in dissipative isotropic media, the group velocity loses its physical meaning, and the energy velocity equals the phase velocity only for homogeneous viscoelastic plane waves. In this section, we investigate the relations between the different velocities for SH homogeneous viscoelastic plane waves. Moreover, we study the perpendicularity properties – shown to hold for elastic media (see Section 1.4.6) – between slowness surface and energy-velocity vector, and between wave or ray surface and slowness vector.

4.4.1 Energy velocity

Let us first obtain the relation between the energy velocity and the envelope velocity, as defined in equation (1.146) for the (x, z) -plane. Differentiating equation (4.78) with respect to the propagation – or attenuation – angle θ , squaring it and adding the result to the square of equation (4.78), we obtain

$$v_e^2 = v_{env}^2 - \frac{d\mathbf{v}_e}{d\theta} \cdot \hat{\boldsymbol{\kappa}} \left(\frac{d\mathbf{v}_e}{d\theta} \cdot \hat{\boldsymbol{\kappa}} + 2 \frac{d\hat{\boldsymbol{\kappa}}}{d\theta} \cdot \mathbf{v}_e \right), \quad (4.104)$$

where we have used the relations $d\hat{\boldsymbol{\kappa}}/d\theta = (l_3, -l_1)$, $l_1^2 + l_3^2 = 1$, and $l_1 = \sin \theta$ and $l_3 = \cos \theta$ are the direction cosines.

The dispersion relation for SH propagation in the symmetry plane of a monoclinic medium can be expressed as

$$p_{66}l_1^2 + p_{44}l_3^2 - \rho v_c^2 = 0, \quad (4.105)$$

where v_c is the corresponding complex velocity. Since the complex-slowness vector for homogeneous plane waves is $\mathbf{s} = \mathbf{k}/\omega = (s_1, s_3)\hat{\boldsymbol{\kappa}}$, equation (4.105) generalizes equations (1.261) to the lossy case – an appropriate rotation of coordinates eliminates the stiffness p_{46} . The solution of equation (4.105) is

$$v_c = \sqrt{\frac{p_{66}l_1^2 + p_{44}l_3^2}{\rho}}. \quad (4.106)$$

The displacement field has the following form

$$\mathbf{u} = \hat{\mathbf{e}}_2 U_0 \exp[i(\omega t - k_1 x - k_3 z)], \quad (4.107)$$

or

$$\mathbf{u} = \hat{\mathbf{e}}_2 U_0 \exp(-\boldsymbol{\alpha} \cdot \mathbf{x}) \exp[i\omega(t - \mathbf{s}_R \cdot \mathbf{x})], \quad (4.108)$$

where U_0 is a complex quantity, k_1 and k_3 are the components of the complex wavevector \mathbf{k} , and $\mathbf{s}_R = \boldsymbol{\kappa}/\omega$ is the slowness vector.

The associated strain components are

$$\begin{aligned} e_4 &= \partial_3 u = -ik_3 U_0 \exp[i(\omega t - \mathbf{k} \cdot \mathbf{x})], \\ e_6 &= \partial_1 u = -ik_1 U_0 \exp[i(\omega t - \mathbf{k} \cdot \mathbf{x})], \end{aligned} \quad (4.109)$$

and the stress components are

$$\begin{aligned}\sigma_4 &= p_{44}e_4 = -ip_{44}k_3U_0 \exp[i(\omega t - \mathbf{k} \cdot \mathbf{x})], \\ \sigma_6 &= p_{66}e_6 = -ip_{66}k_1U_0 \exp[i(\omega t - \mathbf{k} \cdot \mathbf{x})].\end{aligned}\quad (4.110)$$

From equation (4.55), the Umov-Poynting vector is

$$\mathbf{p} = -\frac{1}{2}v^*(\sigma_4\hat{\mathbf{e}}_3 + \sigma_6\hat{\mathbf{e}}_1) = \frac{1}{2v_c}\omega^2|U_0|^2(l_3p_{44}\hat{\mathbf{e}}_3 + l_1p_{66}\hat{\mathbf{e}}_1)\exp(-2\alpha \cdot \mathbf{x}), \quad (4.111)$$

where $v = i\omega u$ is the particle velocity. Note that for elastic media, the Umov-Poynting vector is real because v_c , p_{44} and p_{66} become real valued.

The time-averaged kinetic-energy density is, from equation (4.52),

$$\langle T \rangle = \frac{1}{4}\rho\mathbf{v}^* \cdot \mathbf{v} = \frac{1}{4}\rho\omega^2|U_0|^2 \exp(-2\alpha \cdot \mathbf{x}), \quad (4.112)$$

and the time-averaged strain-energy density is, from equation (4.53),

$$\langle V \rangle = \frac{1}{4}\text{Re}(p_{44}|e_4|^2 + p_{66}|e_6|^2) = \frac{1}{4}\rho\omega^2|U_0|^2 \frac{\text{Re}(v_c^2)}{|v_c|^2} \exp(-2\alpha \cdot \mathbf{x}), \quad (4.113)$$

where equations (4.28) and (4.106) have been used. Similarly, the time average of the rate of dissipated-energy density (4.54) is

$$\langle \dot{D} \rangle = \frac{1}{2}\rho\omega^3|U_0|^2 \frac{\text{Im}(v_c^2)}{|v_c|^2} \exp(-2\alpha \cdot \mathbf{x}). \quad (4.114)$$

As can be seen from equations (4.112) and (4.113), the two time-averaged energy densities are identical for elastic media, because v_c is real. For anelastic media, the difference between them is given by the factor $\text{Re}(v_c^2)/|v_c|^2$ in the strain-energy density. Since the property (4.42) can be applied to homogeneous plane waves, we have $T_{\text{peak}} = 2\langle T \rangle$ and $V_{\text{peak}} = 2\langle V \rangle$.

Substitution of the Umov-Poynting vector and energy densities into equation (4.76) gives the energy velocity for SH waves, namely,

$$\mathbf{v}_e = \frac{v_p}{\text{Re}(v_c)} \left[l_1 \text{Re} \left(\frac{p_{66}}{\rho v_c} \right) \hat{\mathbf{e}}_1 + l_3 \text{Re} \left(\frac{p_{44}}{\rho v_c} \right) \hat{\mathbf{e}}_3 \right]. \quad (4.115)$$

Note the difference from the energy velocity (1.154) in the elastic case, for which $v_c = v_p$.

4.4.2 Group velocity

Using equation (4.28) and noting that $k_1 = kl_1$ and $k_3 = kl_3$ for homogeneous plane waves, we can rewrite the complex dispersion relation (4.105) as

$$F(k_1, k_3, \omega) = p_{66}k_1^2 + p_{44}k_3^2 - \rho\omega^2 = 0. \quad (4.116)$$

The group velocity (4.39) can be computed using this implicit relation between ω and the real wavenumber components κ_1 and κ_3 . The partial derivatives are given by

$$\frac{\partial F}{\partial k_1} = 2p_{66}k_1, \quad \frac{\partial F}{\partial k_3} = 2p_{44}k_3, \quad (4.117)$$

and

$$\frac{\partial F}{\partial \omega} = p_{66,\omega} k_1^2 + p_{44,\omega} k_3^2 - 2\rho\omega, \quad (4.118)$$

where the subscript ω denotes the derivative with respect to ω . Consequently, substituting these expressions into equation (4.39), we get

$$\mathbf{v}_g = -2l_1 \left[\operatorname{Re} \left(\frac{d}{v_c p_{66}} \right) \right]^{-1} \hat{\mathbf{e}}_1 - 2l_3 \left[\operatorname{Re} \left(\frac{d}{v_c p_{44}} \right) \right]^{-1} \hat{\mathbf{e}}_3, \quad (4.119)$$

where

$$d = \omega(p_{66,\omega} l_1^2 + p_{44,\omega} l_3^2) - 2\rho v_c^2. \quad (4.120)$$

Comparison of equations (4.115) and (4.119) indicates that the energy velocity is not equal to the group velocity for all frequencies. The group velocity has physical meaning only for low-loss media as an approximation to the energy velocity. It is easy to verify that the two velocities coincide for lossless media.

4.4.3 Envelope velocity

Differentiating the phase velocity (4.29) (by using equation (4.106)), and substituting the result into equation (1.146), we obtain the magnitude of the envelope velocity:

$$v_{env} = v_p \sqrt{1 + l_1^2 l_3^2 v_p^2 \left[\operatorname{Re} \left(\frac{p_{66} - p_{44}}{\rho v_c^3} \right) \right]^2}. \quad (4.121)$$

If the medium is isotropic, $p_{66} = p_{44}$, and the envelope velocity equals the phase velocity and the energy velocity (4.115). For lossless media $p_{IJ} = c_{IJ}$ (the elasticity constants) are real quantities, $v_p = v_c$, and

$$v_{env} = v_e = v_g = \frac{1}{\rho v_p} \sqrt{c_{66}^2 l_1^2 + c_{44}^2 l_3^2} \quad (4.122)$$

(see equation (1.149)).

4.4.4 Perpendicularity properties

In anisotropic elastic media, the energy velocity is perpendicular to the slowness surface and the wavevector is perpendicular to the energy-velocity surface or wave surface (see Section 1.4.6). These properties do not apply, in general, to anisotropic anelastic media as will be seen in the following derivations. The equation of the slowness curve can be obtained by using the dispersion relation (4.105). Dividing the slowness $s_R = 1/\operatorname{Re}(v_c)$ by s_R and using $s_{R1} = s_R l_1$ and $s_{R3} = s_R l_3$, we obtain the equation for the slowness curve, namely,

$$\Omega(s_{R1}, s_{R3}) = \operatorname{Re} \left[\left(\frac{s_{R1}^2}{\rho/p_{66}} + \frac{s_{R3}^2}{\rho/p_{44}} \right)^{-1/2} \right] - 1 = 0. \quad (4.123)$$

A vector perpendicular to this curve is given by

$$\nabla_{s_R} \Omega = \left(\frac{\partial \Omega}{\partial s_{R1}}, \frac{\partial \Omega}{\partial s_{R3}} \right) = -v_p^2 \left[l_1 \operatorname{Re} \left(\frac{p_{66}}{\rho v_c^3} \right) \hat{\mathbf{e}}_1 + l_3 \operatorname{Re} \left(\frac{p_{44}}{\rho v_c^3} \right) \hat{\mathbf{e}}_3 \right]. \quad (4.124)$$

It is clear from equation (4.115) that \mathbf{v}_e and $\nabla_{s_R}\Omega$ are not collinear vectors; thus, the energy velocity is not perpendicular to the slowness surface. However, if we consider the limit $\omega \rightarrow \infty$ – the elastic, lossless limit by convention – for which $p_{IJ} \rightarrow c_{IJ}$, we may state that in this limit, the energy-velocity vector is perpendicular to the unrelaxed slowness surface. The same perpendicularity properties hold for the static limit ($\omega \rightarrow 0$).

Similarly, the other perpendicularity property of elastic media, i.e., that the slowness vector must be perpendicular to the energy-velocity surface, is not valid for anelastic media at all frequencies. By using equation (4.29), and differentiating equation (4.78) with respect to θ , we obtain

$$\frac{d\kappa}{d\theta} \cdot \mathbf{v}_e + \kappa \cdot \frac{d\mathbf{v}_e}{d\theta} = \frac{d\kappa}{d\theta} \cdot \mathbf{v}_e + \varrho \kappa \cdot \frac{d\mathbf{v}_e}{d\phi} = 0, \quad (4.125)$$

where $\varrho = d\phi/d\theta$, with

$$\tan \phi = \frac{v_{e1}}{v_{e3}} = \frac{\text{Re}[p_{66}/v_c(\theta)]}{\text{Re}[p_{44}/v_c(\theta)]} \tan \theta \quad (4.126)$$

(from equation (4.115)).

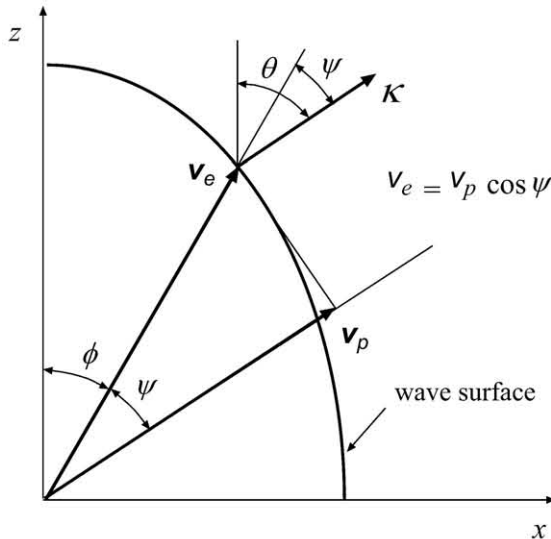


Figure 4.3: Relation between the energy velocity and the phase velocity in terms of the propagation and energy angles.

Figure 4.3 shows the relation between the propagation and energy angles. It can be shown that ϱ is always different from zero, in particular $\varrho = 1$ for isotropic media. Since $d\kappa/d\theta$ is tangent to the slowness surface – recall that $\kappa = \omega s_R$ – and \mathbf{v}_e is not perpendicular to it, the first term in equation (4.125) is different from zero. Since $d\mathbf{v}_e/d\phi$ is tangent to the wave surface, equation (4.125) implies that the real wavevector κ is not perpendicular to that surface. In fact, taking into account that $\kappa(\theta) = [\omega/v_p(\theta)](\sin(\theta)\hat{e}_1 +$

$\cos(\theta)\hat{\mathbf{e}}_3$), and after a lengthy but straightforward calculation of the first term of equation (4.125), we have

$$\frac{d\boldsymbol{\kappa}}{d\theta} \cdot \mathbf{v}_e = \omega v_p l_1 l_3 \operatorname{Re} \left[\frac{(p_{66} - p_{44})}{\rho v_c} \left(\frac{1}{|v_c|^2} - \frac{1}{v_c^2} \right) \right]. \quad (4.127)$$

For lossless media, v_c is real and equation (4.127) is identically zero; in this case, the perpendicularity properties are verified:

$$\frac{d\mathbf{v}_e}{d\theta} \cdot \boldsymbol{\kappa} = \frac{d\boldsymbol{\kappa}}{d\theta} \cdot \mathbf{v}_e = 0, \quad (4.128)$$

and from equation (4.104) the envelope velocity equals the energy velocity. In lossless media or at the unrelaxed and static limits in lossy media, the wavevector is perpendicular to the wave surface – the wave front in the unrelaxed case.

Perpendicularity for all frequencies in anelastic media holds between the slowness surface and the envelope-velocity vector, as well as the surface determined by the envelope-velocity vector and the slowness vector. Using equations (1.142), (4.29) and (4.106), we obtain the components of the envelope velocity,

$$v_{env})_1 = v_p^2 l_1 \operatorname{Re} \left(\frac{p_{66}}{\rho v_c^3} \right), \quad \text{and} \quad v_{env})_3 = v_p^2 l_3 \operatorname{Re} \left(\frac{p_{44}}{\rho v_c^3} \right). \quad (4.129)$$

The associated vector is collinear to $\nabla_{s_R} \Omega$ for all frequencies (see equation (4.124)). Moreover, since the expression of the envelope of plane waves has the same form as in the elastic case (equation (1.165)), the same reasoning used in Section 1.4.6 implies that the real wavenumber vector and the slowness vector are perpendicular to the surface defined by the envelope velocity.

4.4.5 Numerical evaluation of the energy velocity

Let us compare the different physical velocities. Figure 4.4 compares a numerical evaluation of the location of the energy (white dots) and the theoretical energy velocity (solid curve). The energy velocity is computed from the snapshot by finding the baricenter of $|\mathbf{u}|^2$ along the radial direction. Attenuation is modeled by Zener elements for which the characteristic frequency coincides with the source dominant frequency.

This comparison is represented in a linear plot in Figure 4.5, where the envelope and group velocities are also represented. While the envelope and energy velocities practically coincide, the group velocity gives a wrong prediction of the energy location. More details about this comparison are given in Carcione, Quiroga-Goode and Cavallini (1996). Carcione (1994a) also considers the qP-qS case.

It is important to note here that there exist conditions under which the group velocity has a clear physical meaning. The concept of signal velocity introduced by Sommerfeld and Brillouin (Brillouin, 1960; Mainardi, 1983) describes the velocity of energy transport for the Lorentz model. It is equal to the group velocity in regions of dispersion without attenuation (Felsen and Marcuvitz, 1973; Mainardi, 1987; Oughstun and Sherman, 1994). This happens, under certain conditions, in the process of resonance attenuation in solid, liquid and gaseous media. The Lorentz model describes dielectric-type media as a set of

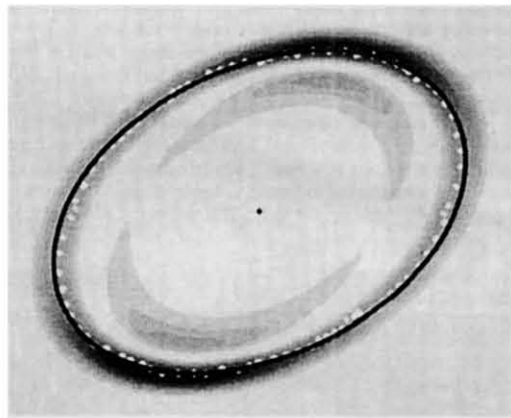


Figure 4.4: Comparison between a numerical evaluation of the energy location (white dots) and the theoretical energy-velocity curve (solid line). The former is computed by finding the center of gravity of the energy-like quantity $|u|^2$ along the radial direction.

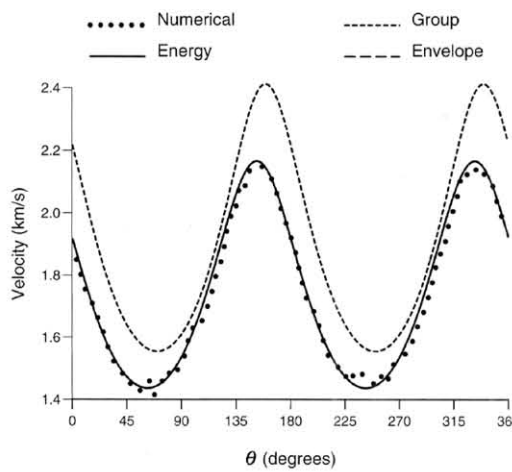


Figure 4.5: Same comparison as in Figure 4.4, but here the envelope and group velocities are also represented. The dotted line corresponds to the numerical evaluation of the energy velocity and θ is the propagation angle.

neutral atoms with “elastically” bound electrons to the nucleus, where each electron is bound by a Hooke’s law restoring force (Nussenzveig, 1972; Oughstun and Sherman, 1994). The atoms vibrate at a resonance frequency under the action of an electromagnetic field. This process implies attenuation and dispersion, since the electrons emit electromagnetic waves which carry away energy.

Garret and McCumber (1970) and Steinberg and Chiao (1994) show that the group velocity describes the velocity of the pulse for electromagnetic media such as, for example, gain-assisted linear anomalous dispersion in cesium gas. Basically, the conditions imply that the group velocity remains constant over the pulse bandwidth so that the light pulse maintains its shape during the propagation. These theoretical results are confirmed by Wang, Kuzmich and Dogariu (2000), who report a very large superluminal effect for laser pulses of visible light, in which a pulse propagates with a negative group velocity without violating causality.

However, the classical concepts of phase, energy and group velocities generally break down for the Lorentz model, depending on the value of the source dominant frequency and source bandwidth compared to the width of the spectral line. Loudon (1970) has derived an expression of the energy velocity which does not exceed the velocity of light. It is based on the fact that when the frequency of the wave is close to the oscillator frequency, part of the energy resides in the excited oscillators. This part of the energy must be added to the electromagnetic field energy.

4.4.6 Forbidden directions of propagation

There is a singular phenomenon when inhomogeneous plane waves propagate in a medium with anisotropy and attenuation. The theory predicts, beyond a given degree of inhomogeneity, the existence of forbidden directions (forbidden solutions) or “stop bands” where there is no wave propagation (not to be confused with the frequency stop bands of periodic structures (e.g., Silva, 1991; Carcione and Poletto, 2000)). This phenomenon does not occur in dissipative isotropic and anisotropic elastic media. The combination of anelasticity and anisotropy activates the bands. These solutions are found even in very weakly anisotropic and quasi-elastic materials; only a finite value of Q is required. Weaker anisotropy does not affect the width of the bands, but increases the threshold of inhomogeneity above which they appear; moreover, near the threshold, lower attenuation implies narrower bands.

This phenomenon was discovered by Krebes and Le (1994) and Carcione and Cavallini (1995a) for wave propagation of pure shear inhomogeneous viscoelastic plane waves in the symmetry plane of a monoclinic medium. Carcione and Cavallini (1997) predict the same phenomenon in electromagnetic media on the basis of the acoustic-electromagnetic analogy (Carcione and Cavallini, 1995b). Figure 4.6a-b represents the square of the phase velocity as a function of the propagation angle, where the dashed line corresponds to the homogeneous wave ($\gamma = 0$); (a) and (b) correspond to strong and weak attenuation, respectively. Observe that in the transition from $\gamma = 60^\circ$ to $\gamma = 68^\circ$, two “stop bands” develop (for $\gamma > \gamma_0 \approx 64^\circ$) where the wave does not propagate (Figure 4.6a). Note that the stop bands exist even for high values of Q , as is the case in Figure 4.6b. The behavior is such that these stop bands exist for any finite value of Q , with their width decreasing with increasing Q .

Červený and Pšenčík (2005a,b) have used a form of the sextic Stroh formalism (Ting, 1996; Caviglia and Morro, 1999) to re-interpret the forbidden-directions phenomenon by using a different inhomogeneity parameter, instead of angle γ . The new approach involves the solution of a 6×6 complex-valued eigensystem and the parameterization excludes the forbidden solutions.

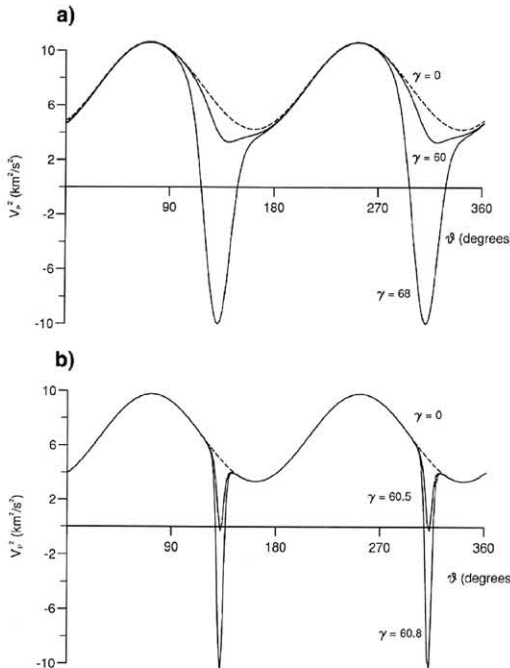


Figure 4.6: “Stopbands” for propagation of inhomogeneous viscoelastic plane waves in anisotropic anelastic media. The figure shows the square of the phase velocity as a function of the propagation angle for different values of the inhomogeneity angle γ . In (a) the medium has strong dissipation and in (b) the dissipation is weak.

4.5 Memory variables and equation of motion in the time domain

As in the isotropic viscoelastic case (Section 3.9), we obtain, in this section, the memory-variable differential equations, which allow us to avoid numerical calculations of time convolutions when modeling wave propagation.

We define the reference elastic limit in the unrelaxed regime ($\omega \rightarrow \infty$ or $t \rightarrow 0$), and denote the unrelaxed stiffnesses by c_{IJ} . The following equations correspond to the 3-D case, but the space dimension is indicated by n instead of 3 to facilitate the particularization to the 2-D case ($n=2$). Using model 3 of Section 4.1.3, the time-domain relaxation

matrix for a medium with general anisotropic properties (a triclinic medium) has the following symmetric form

$$\Psi(t) = \begin{pmatrix} \check{\psi}_{11} & \check{\psi}_{12} & \check{\psi}_{13} & c_{14} & c_{15} & c_{16} \\ \check{\psi}_{21} & \check{\psi}_{22} & \check{\psi}_{23} & c_{24} & c_{25} & c_{26} \\ & \check{\psi}_{31} & \check{\psi}_{32} & c_{34} & c_{35} & c_{36} \\ & & \check{\psi}_{41} & c_{45} & c_{46} & \\ & & & \check{\psi}_{51} & c_{56} & \\ & & & & \check{\psi}_{61} & \end{pmatrix} H(t). \quad (4.130)$$

We may express the components as

$$\check{\psi}_{I(I)} = c_{I(I)} - \bar{\mathcal{E}} + \bar{\mathcal{K}}\chi_1 + 2\left(1 - \frac{1}{n}\right)\bar{\mu}\chi_\delta, \quad I = 1, 2, 3, \quad (4.131)$$

$$\check{\psi}_{IJ} = c_{IJ} - \bar{\mathcal{E}} + \bar{\mathcal{K}}\chi_1 + 2\bar{\mu}\left(1 - \frac{1}{n}\chi_\delta\right), \quad I, J = 1, 2, 3; I \neq J, \quad (4.132)$$

$$\check{\psi}_{44} = c_{44}\chi_2, \quad \check{\psi}_{55} = c_{55}\chi_3, \quad \check{\psi}_{66} = c_{66}\chi_4, \quad (4.133)$$

where

$$\bar{\mathcal{E}} = \bar{\mathcal{K}} + 2\left(1 - \frac{1}{n}\right)\bar{\mu}, \quad (4.134)$$

$$\chi_\nu(t) = L_\nu \left(\sum_{l=1}^{L_\nu} \frac{\tau_{el}^{(\nu)}}{\tau_{\sigma l}^{(\nu)}} \right)^{-1} \left[1 - \frac{1}{L_\nu} \sum_{l=1}^{L_\nu} \left(1 - \frac{\tau_{el}^{(\nu)}}{\tau_{\sigma l}^{(\nu)}} \right) \exp(-t/\tau_{\sigma l}^{(\nu)}) \right], \quad \nu = 1, \dots, 4, \quad (4.135)$$

with $\tau_{el}^{(\nu)}$ and $\tau_{\sigma l}^{(\nu)}$ being relaxation times satisfying $\tau_{el}^{(\nu)} \geq \tau_{\sigma l}^{(\nu)}$. Moreover, $\chi = 1$ for $t = 0$ and $\tau_{el}^{(\nu)} = \tau_{\sigma l}^{(\nu)}$. The index δ can be chosen to be 2, 3 or 4 (see Section 4.1.3).

The complex modulus is the time Fourier transform of $d(\chi_\nu H)/dt$. It yields

$$M_\nu(\omega) = \left(\sum_{l=1}^{L_\nu} \frac{\tau_{el}^{(\nu)}}{\tau_{\sigma l}^{(\nu)}} \right)^{-1} \sum_{l=1}^{L_\nu} \frac{1 + i\omega\tau_{el}^{(\nu)}}{1 + i\omega\tau_{\sigma l}^{(\nu)}} \quad (4.136)$$

(see equation (2.196)), which has the property $M_\nu \rightarrow 1$ for $\omega \rightarrow \infty$.

The relaxation functions (4.135) are sufficiently general to describe any type of frequency behavior of attenuation and velocity dispersion.

4.5.1 Strain memory variables

The time-domain stress-strain relation can be expressed as

$$\sigma_I = \psi_{IJ} * \partial_t e_J \quad (4.137)$$

(see equation (2.22)), where σ_I and e_J are the components of the stress and strain 6×1 arrays – equations (1.20) and (1.27), respectively.

Applying the Boltzmann operation (2.6) to equation (4.137), we obtain

$$\sigma_I = A_{IJ}^{(\nu)} e_J + B_{IJ}^{(\nu)} \sum_{l=1}^{L_\nu} e_{Jl}^{(\nu)}, \quad (4.138)$$

where the A 's and the B 's are combinations of the elasticity constants c_{IJ} , and

$$e_{Jl}^{(\nu)} = \varphi_{\nu l} * e_J, \quad J = 1, \dots, 6, \quad l = 1, \dots, L_\nu, \quad \nu = 1, \dots, 4 \quad (4.139)$$

are the components of the 6×1 strain memory array $\mathbf{e}_l^{(\nu)}$, with

$$\varphi_{\nu l}(t) = \frac{1}{\tau_{\sigma l}^{(\nu)}} \left(\sum_{l=1}^{L_\nu} \frac{\tau_{el}^{(\nu)}}{\tau_{\sigma l}^{(\nu)}} \right)^{-1} \left(1 - \frac{\tau_{el}^{(\nu)}}{\tau_{\sigma l}^{(\nu)}} \right) \exp(-t/\tau_{\sigma l}^{(\nu)}) \quad (4.140)$$

being the response function corresponding to the l -th dissipation mechanism. In 3-D space, the strain memory array is a symmetric tensor given by

$$\mathbf{e}_l^{(\nu)} = \begin{pmatrix} e_{11l}^{(\nu)} & e_{12l}^{(\nu)} & e_{13l}^{(\nu)} \\ e_{21l}^{(\nu)} & e_{22l}^{(\nu)} & e_{23l}^{(\nu)} \\ e_{31l}^{(\nu)} & e_{32l}^{(\nu)} & e_{33l}^{(\nu)} \end{pmatrix} = \varphi_{\nu l} * \mathbf{e}, \quad (4.141)$$

corresponding to the l -th dissipation mechanism of the relaxation function χ_ν . This tensor contains the past history of the material due to that mechanism. In the elastic case ($\tau_{\sigma l}^{(\nu)} \rightarrow \tau_{el}^{(\nu)}$), $\varphi_{\nu l} \rightarrow 0$ and the strain memory tensor vanishes. As the strain tensor, the memory tensor possesses the unique decomposition

$$\mathbf{e}_l^{(\nu)} = \mathbf{d}_l^{(\nu)} + \frac{1}{n} \text{tr}(\mathbf{e}_l^{(\nu)}) \mathbf{I}_n, \quad \text{tr}(\mathbf{d}_l^{(\nu)}) = 0, \quad (4.142)$$

where the traceless symmetric tensor $\mathbf{d}_l^{(\nu)}$ is the deviatoric strain memory tensor. Then, the dilatational and shear memory variables can be defined as

$$e_{1l} = \text{tr}(\mathbf{e}_l^{(1)}) \quad \text{and} \quad e_{ijl}^{(\nu)} = \left(\mathbf{d}_l^{(\nu)} \right)_{ij}, \quad (4.143)$$

respectively, where $\nu = \delta$ for $i = j$, $\nu = 2$ for $ij = 23$, $\nu = 3$ for $ij = 13$, and $\nu = 4$ for $ij = 12$.

In explicit form, the stress-strain relations in terms of the strain components and memory variables are

$$\begin{aligned} \sigma_1 &= c_{1J} e_J + \bar{K} \sum_{l=1}^{L_1} e_{1l} + 2\bar{\mu} \sum_{l=1}^{L_\delta} e_{11l}^{(\delta)} \\ \sigma_2 &= c_{2J} e_J + \bar{K} \sum_{l=1}^{L_1} e_{1l} + 2\bar{\mu} \sum_{l=1}^{L_\delta} e_{22l}^{(\delta)} \\ \sigma_3 &= c_{3J} e_J + \bar{K} \sum_{l=1}^{L_1} e_{1l} - 2\bar{\mu} \sum_{l=1}^{L_\delta} (e_{11l}^{(\delta)} + e_{22l}^{(\delta)}) \\ \sigma_4 &= c_{4J} e_J + c_{44} \sum_{l=1}^{L_2} e_{23l}^{(2)} \\ \sigma_5 &= c_{5J} e_J + c_{55} \sum_{l=1}^{L_3} e_{13l}^{(3)} \\ \sigma_6 &= c_{6J} e_J + c_{66} \sum_{l=1}^{L_4} e_{12l}^{(4)} \end{aligned} \quad (4.144)$$

where, as stated before,

$$c_{IJ} = \psi_{IJ}(t = 0^+) \quad (4.145)$$

are the unrelaxed elasticity constants. In the work of Carcione (1995), the memory variables are multiplied by relaxed elasticity constants. This is due to a different definition of the response function (4.140). For instance, in the 1-D case with one dissipation mechanism (see equations (2.283) and (2.285)), the difference is the factor $\tau_\epsilon/\tau_\sigma$.

The terms containing the stress components describe the instantaneous (unrelaxed) response of the medium, and the terms involving the memory variables describe the previous states of deformation. Note that because $\mathbf{d}_l^{(\nu)}$ is traceless, $e_{11l}^{(\delta)} + e_{22l}^{(\delta)} + e_{33l}^{(\delta)} = 0$, and the number of independent variables is six, i.e., the number of strain components. The nature of the terms can be easily identified: in the diagonal stress components, the dilatational memory variables are multiplied by a generalized bulk modulus $\bar{\mathcal{K}}$, and the shear memory variables are multiplied by a generalized rigidity modulus $\bar{\mu}$.

4.5.2 Memory-variable equations

Application of the Boltzmann operation (2.6) to the deviatoric part of equation (4.141) gives

$$\partial_t \mathbf{d}_l^{(\nu)} = \varphi_{\nu l}(0)\mathbf{d} + (\partial_t \check{\varphi}_{\nu l} H) * \mathbf{d}, \quad (4.146)$$

where \mathbf{d} is the deviatoric strain tensor whose components are given in equation (1.15). Because $\partial_t \check{\varphi}_{\nu l} = -\check{\varphi}_{\nu l}/\tau_{\sigma l}^{(\nu)}$, equation (4.146) becomes

$$\partial_t \mathbf{d}_l^{(\nu)} = \varphi_{\nu l}(0)\mathbf{d} - \frac{1}{\tau_{\sigma l}^{(\nu)}} \mathbf{d}_l^{(\nu)}, \quad \mathbf{d}_l^{(\nu)} = \varphi_{\nu l} * \mathbf{d}, \quad \nu = 2, 3, 4. \quad (4.147)$$

Similarly, applying the Boltzmann operation to $\text{tr}(\mathbf{e}_l^{(1)})$, we obtain

$$\partial_t \text{tr}(\mathbf{e}_l^{(1)}) = \varphi_{1l}(0)\text{tr}(\mathbf{e}) - \frac{1}{\tau_{\sigma l}^{(1)}} \text{tr}(\mathbf{e}_l^{(1)}). \quad (4.148)$$

The explicit equations in terms of the memory variables are

$$\begin{aligned} \partial_t e_{1l} &= n\varphi_{1l}(0)\bar{\epsilon} - \frac{1}{\tau_{\sigma l}^{(1)}} e_{1l}, \quad l = 1, \dots, L_1 \\ \partial_t e_{11l}^{(\delta)} &= \varphi_{\delta l}(0)(e_{11}^{(\delta)} - \bar{\epsilon}) - \frac{1}{\tau_{\sigma l}^{(\delta)}} e_{11l}^{(\delta)}, \quad l = 1, \dots, L_\delta \\ \partial_t e_{22l}^{(\delta)} &= \varphi_{\delta l}(0)(e_{22}^{(\delta)} - \bar{\epsilon}) - \frac{1}{\tau_{\sigma l}^{(\delta)}} e_{22l}^{(\delta)}, \quad l = 1, \dots, L_\delta \\ \partial_t e_{23l} &= \varphi_{2l}(0)e_{23} - \frac{1}{\tau_{\sigma l}^{(2)}} e_{23l}, \quad l = 1, \dots, L_2 \\ \partial_t e_{13l} &= \varphi_{3l}(0)e_{13} - \frac{1}{\tau_{\sigma l}^{(3)}} e_{13l}, \quad l = 1, \dots, L_3 \\ \partial_t e_{12l} &= \varphi_{4l}(0)e_{12} - \frac{1}{\tau_{\sigma l}^{(4)}} e_{12l}, \quad l = 1, \dots, L_4, \end{aligned} \quad (4.149)$$

where $\bar{\epsilon} = e_{II}/n$. The index δ can be chosen to be 2, 3 or 4 (see Section 4.1.3).

Two different formulations of the anisotropic viscoelastic equation of motion follow. In the displacement formulation, the unknown variables are the displacement field and the memory variables. In this case, the equation of motion is formulated using the strain-displacement relations (1.2), the stress-strain relations (4.144), the equations of momentum conservation (1.23) and the memory-variable equations (4.149). In the particle-velocity/stress formulation, the field variables are the particle velocities, the stress components and the time derivative of the memory variables, because the first time derivative

of the stress-strain relations are required. The first formulation is second-order in the time derivatives, while the second is first-order. In the particle-velocity/stress formulation case, the material properties are not differentiated explicitly, as they are in the displacement formulation. A practical example of 3-D viscoelastic anisotropic modeling applied to an exploration-geophysics problem is given by Dong and McMechan (1995).

2-D equations of motion – referred to as SH and qP-qSV equations of motion – can be obtained if the material properties are uniform in the direction perpendicular to the plane of wave propagation. Alternatively, the decoupling occurs in three dimensions in a symmetry plane. This situation can be generalized up to monoclinic media provided that the plane of propagation is the plane of symmetry of the medium. In fact, propagation in the plane of mirror symmetry of a monoclinic medium is the most general situation for which pure shear waves exist at all propagation angles.

Alternative methods for simulating wave propagation in anisotropic media – including attenuation effects – are based on ray-tracing algorithms. Gajewski, and Pšenčík (1992) use the ray method for weakly anisotropic media, and Le, Krebes and Quiroga-Goode (1994) simulate SH-wave propagation by complex ray tracing.

4.5.3 SH equation of motion

Let us assume that the (x, z) -plane is the symmetry plane of a monoclinic medium and $\partial_2 = 0$. The cross-plane assumption implies that the only non-zero stress components are σ_{12} and σ_{23} . Following the same steps to obtain the 3-D equation of motion, the displacement formulation of the SH-equation of motion is given by

- i) Euler's equation $(1.46)_1$.
- ii) The stress-strain relations

$$\begin{aligned}\sigma_4 &= c_{44}e_4 + c_{46}e_6 + c_{44} \sum_{l=1}^{L_2} e_{23l}, \\ \sigma_6 &= c_{46}e_4 + c_{66}e_6 + c_{66} \sum_{l=1}^{L_4} e_{12l}.\end{aligned}\quad (4.150)$$

- iii) Equations $(4.149)_4$ and $(4.149)_6$.

See Carcione and Cavallini (1995c) for more details about this wave equation.

4.5.4 qP-qSV equation of motion

Let us consider the two-dimensional particle-velocity/stress equations for propagation in the (x, z) -plane of a transversely isotropic medium. In this case, we explicitly consider a two-dimensional world, i.e., $n = 2$. We assign one relaxation mechanism to dilatational anelastic deformations ($\nu = 1$) and one relaxation mechanism to shear anelastic deformations ($\nu = 2$). The equations governing wave propagation can be expressed by

- i) Euler's equations $(1.45)_1$ and $(1.45)_2$:

$$\partial_1\sigma_{11} + \partial_3\sigma_{13} + f_1 = \rho\partial_t v_1, \quad (4.151)$$

$$\partial_1\sigma_{13} + \partial_3\sigma_{33} + f_3 = \rho\partial_t v_3, \quad (4.152)$$

where f_1 and f_3 are the body-force components.

- ii) Stress-strain relations:

$$\partial_t \sigma_{11} = c_{11} \partial_1 v_1 + c_{13} \partial_3 v_3 + \bar{\mathcal{K}} \epsilon_1 + 2c_{55} \epsilon_2, \quad (4.153)$$

$$\partial_t \sigma_{33} = c_{13} \partial_1 v_1 + c_{33} \partial_3 v_3 + \bar{\mathcal{K}} \epsilon_1 - 2c_{55} \epsilon_2, \quad (4.154)$$

$$\partial_t \sigma_{13} = c_{55} [(\partial_3 v_1 + \partial_1 v_3) + \epsilon_3], \quad (4.155)$$

where ϵ_1 , ϵ_2 and ϵ_3 are first time derivatives of the memory variables ($\partial_t e_{11}$, $\partial_t e_{22}$ and $\partial_t e_{13}$, respectively), and

$$\bar{\mathcal{K}} = \bar{\mathcal{E}} - c_{55}, \quad \bar{\mathcal{E}} = \frac{1}{2}(c_{11} + c_{33}). \quad (4.156)$$

As in the 3-D case, the stress-strain relations satisfy the condition that the mean stress depends only on the dilatational relaxation function in any coordinate system – the trace of the stress tensor should be invariant under coordinate transformations. Moreover, the deviatoric stresses solely depend on the shear relaxation function.

iii) Memory-variable equations:

$$\partial_t \epsilon_1 = \frac{1}{\tau_\sigma^{(1)}} \left[\left(\frac{\tau_\sigma^{(1)}}{\tau_\epsilon^{(1)}} - 1 \right) (\partial_1 v_1 + \partial_3 v_3) - \epsilon_1 \right], \quad (4.157)$$

$$\partial_t \epsilon_2 = \frac{1}{2\tau_\sigma^{(2)}} \left[\left(\frac{\tau_\sigma^{(2)}}{\tau_\epsilon^{(2)}} - 1 \right) (\partial_1 v_1 - \partial_3 v_3) - 2\epsilon_2 \right], \quad (4.158)$$

$$\partial_t \epsilon_3 = \frac{1}{\tau_\sigma^{(2)}} \left[\left(\frac{\tau_\sigma^{(2)}}{\tau_\epsilon^{(2)}} - 1 \right) (\partial_3 v_1 + \partial_1 v_3) - \epsilon_3 \right]. \quad (4.159)$$

Transforming the memory-variable equations (4.157), (4.158) and (4.159) to the ω -domain (e.g., $\partial_t \epsilon_1 \rightarrow i\omega \epsilon_1$), and substituting the memory variables into equations (4.153), (4.154) and (4.155), we obtain the frequency-domain stress-strain relation:

$$i\omega \begin{pmatrix} \sigma_{11} \\ \sigma_{33} \\ \sigma_{13} \end{pmatrix} = \begin{pmatrix} p_{11} & p_{13} & 0 \\ p_{13} & p_{33} & 0 \\ 0 & 0 & p_{55} \end{pmatrix} \cdot \begin{pmatrix} \partial_1 v_1 \\ \partial_3 v_3 \\ \partial_3 v_1 + \partial_1 v_3 \end{pmatrix}, \quad (4.160)$$

where

$$\begin{aligned} p_{11} &= c_{11} - \bar{\mathcal{E}} + \bar{\mathcal{K}} M_1 + c_{55} M_2 \\ p_{33} &= c_{33} - \bar{\mathcal{E}} + \bar{\mathcal{K}} M_1 + c_{55} M_2 \\ p_{13} &= c_{13} - \bar{\mathcal{E}} + \bar{\mathcal{K}} M_1 + c_{55} (2 - M_2) \\ p_{55} &= c_{55} M_2 \end{aligned} \quad (4.161)$$

are the complex stiffnesses, and

$$M_\nu = \frac{\tau_\sigma^{(\nu)}}{\tau_\epsilon^{(\nu)}} \left(\frac{1 + i\omega \tau_\epsilon^{(\nu)}}{1 + i\omega \tau_\sigma^{(\nu)}} \right), \quad \nu = 1, 2 \quad (4.162)$$

are the Zener complex moduli. Note that when $\omega \rightarrow \infty$, $p_{IJ} \rightarrow c_{IJ}$.

The relaxation times can be expressed as (see Section 2.4.5)

$$\tau_\epsilon^{(\nu)} = \frac{\tau_0}{Q_{0\nu}} \left(\sqrt{Q_{0\nu}^2 + 1} + 1 \right), \quad \text{and} \quad \tau_\sigma^{(\nu)} = \frac{\tau_0}{Q_{0\nu}} \left(\sqrt{Q_{0\nu}^2 + 1} - 1 \right), \quad (4.163)$$

where τ_0 is a relaxation time such that $1/\tau_0$ is the center frequency of the relaxation peak and $Q_{0\nu}$ are the minimum quality factors.

4.6 Analytical solution for SH waves in monoclinic media

The following is an example of the use of the correspondence principle to obtain a transient solution in anisotropic anelastic media, where an analytical solution is available in the frequency domain.

In the plane of mirror symmetry of a lossless monoclinic medium, say, the (x, z) -plane, the relevant stiffness matrix describing wave propagation of the cross-plane shear wave is

$$\mathbf{C} = \begin{pmatrix} c_{44} & c_{46} \\ c_{46} & c_{66} \end{pmatrix}. \quad (4.164)$$

Substitution of the stress-strain relation based on (4.164) into Euler's equation (1.46)₁ gives

$$\nabla \cdot \mathbf{C} \cdot \nabla u - \rho \partial_{tt}^2 u = f_u, \quad (4.165)$$

where u is the displacement field, $f_u = -f_2$ is the body force, and, here,

$$\nabla = \begin{pmatrix} \partial_3 \\ \partial_1 \end{pmatrix}. \quad (4.166)$$

For a homogeneous medium, equation (4.165) becomes

$$(c_{44}\partial_3\partial_3 + c_{46}\partial_1\partial_3 + c_{66}\partial_1\partial_1)u - \rho \partial_{tt}^2 u = f_u. \quad (4.167)$$

We show below that it is possible to transform the spatial differential operator on the left-hand side of equation (4.167) to a pure Laplacian differential operator. In that case, equation (4.165) becomes

$$(\partial_{3'}\partial_{3'} + \partial_{1'}\partial_{1'})u - \rho \partial_{tt}^2 u = f, \quad (4.168)$$

where x' and z' are the new coordinates. Considering the solution for the Green function – the right-hand side of (4.168) is Dirac's function in time and space at the origin – and transforming the wave equation to the frequency domain, we obtain

$$(\partial_{3'}\partial_{3'} + \partial_{1'}\partial_{1'})\tilde{g} + \rho\omega^2\tilde{g} = -4\pi\delta(x')\delta(z'), \quad (4.169)$$

where \tilde{g} is the Fourier transform of the Green function, and the constant -4π is introduced for convenience. The solution of (4.169) is

$$\tilde{g}(x', z', \omega) = -i\pi H_0^{(2)}(\sqrt{\rho\omega}r'), \quad (4.170)$$

(see Section 3.10.1), where $H_0^{(2)}$ is the Hankel function of the second kind, and

$$r' = \sqrt{x'^2 + z'^2} = \sqrt{\mathbf{x}'^\top \cdot \mathbf{x}'}, \quad (4.171)$$

with $\mathbf{x}' = (z', x')$. We need to compute (4.170) in terms of the original position vector $\mathbf{x} = (z, x)$. Matrix \mathbf{C} may be decomposed as $\mathbf{C} = \mathbf{A} \cdot \Lambda \cdot \mathbf{A}^\top$, where Λ is the diagonal

matrix of the eigenvalues, and \mathbf{A} is the matrix of the normalized eigenvectors. Thus, the Laplacian operator in (4.165) becomes

$$\nabla \cdot \mathbf{C} \cdot \nabla = \nabla \cdot \mathbf{A} \cdot \boldsymbol{\Lambda} \cdot \mathbf{A}^\top \cdot \nabla = \nabla \cdot \mathbf{A} \cdot \boldsymbol{\Omega} \cdot \boldsymbol{\Omega} \cdot \mathbf{A}^\top \cdot \nabla = \nabla' \cdot \nabla', \quad (4.172)$$

where $\boldsymbol{\Lambda} = \boldsymbol{\Omega}^2$, and

$$\nabla' = \boldsymbol{\Omega} \cdot \mathbf{A}^\top \cdot \nabla. \quad (4.173)$$

Recalling that $\boldsymbol{\Omega}$ is diagonal and $\mathbf{A}^\top = \mathbf{A}^{-1}$, we get

$$\mathbf{x}' = \boldsymbol{\Omega}^{-1} \cdot \mathbf{A}^\top \cdot \mathbf{x}. \quad (4.174)$$

The substitution of (4.174) into equation (4.171) squared gives

$$r'^2 = \mathbf{x} \cdot \mathbf{A} \cdot \boldsymbol{\Omega}^{-1} \cdot \boldsymbol{\Omega}^{-1} \cdot \mathbf{A}^\top \cdot \mathbf{x} = \mathbf{x} \cdot \mathbf{A} \cdot \boldsymbol{\Lambda}^{-1} \cdot \mathbf{A}^\top \cdot \mathbf{x}. \quad (4.175)$$

Since $\mathbf{A} \cdot \boldsymbol{\Lambda}^{-1} \cdot \mathbf{A}^\top = \mathbf{C}^{-1}$, we finally have

$$r'^2 = \mathbf{x} \cdot \mathbf{C}^{-1} \cdot \mathbf{x}^{-1} = (c_{66}z^2 + c_{44}x^2 - 2c_{46}xz)/c, \quad (4.176)$$

where c is the determinant of \mathbf{C} .

Then, substituting (4.176) into equation (4.170), we note that the elastic Green's function becomes

$$\tilde{g}(x, z, \omega) = -i\pi H_0^{(2)} \left(\omega \sqrt{\mathbf{x} \cdot \rho \mathbf{C}^{-1} \cdot \mathbf{x}} \right). \quad (4.177)$$

Application of the correspondence principle (see Section 3.6) gives the viscoelastic Green's function

$$\tilde{g}(x, z, \omega) = -i\pi H_0^{(2)} \left(\omega \sqrt{\mathbf{x} \cdot \rho \mathbf{P}^{-1} \cdot \mathbf{x}} \right), \quad (4.178)$$

where \mathbf{P} is the complex and frequency-dependent stiffness matrix. When solving the problem with a band-limited wavelet $f(t)$, the solution is

$$\tilde{u}(\mathbf{x}, \omega) = -i\pi \tilde{f} H_0^{(2)} \left(\omega \sqrt{\mathbf{x} \cdot \rho \mathbf{P}^{-1} \cdot \mathbf{x}} \right), \quad (4.179)$$

where \tilde{f} is the Fourier transform of f . To ensure a time-domain real solution, when $\omega > 0$ we take

$$\tilde{u}(\mathbf{x}, \omega) = \tilde{u}^*(\mathbf{x}, -\omega), \quad (4.180)$$

where the superscript * denotes the complex conjugate. Finally, the time-domain solution is obtained by an inverse transform based on the discrete fast Fourier transform. An example where dissipation is modeled with Zener models can be found in Carcione and Cavallini (1994a). Other investigations about anisotropy and loss of SH waves are published by Le (1993) and Le, Krebes and Quiroga-Goode (1994).